AWARD NUMBER: W81XWH-15-1-0411

TITLE: Central Tolerance Blockade to Augment Checkpoint Immunotherapy in Melanoma

PRINCIPAL INVESTIGATOR: Maureen Su, MD

CONTRACTING ORGANIZATION: The University of North Carolina at Chapel Hill
Chapel Hill, NC 27599-7280

REPORT DATE: NOVEMBER 2018

TYPE OF REPORT: Final

PREPARED FOR: U.S. Army Medical Research and Materiel Command
Fort Detrick, Maryland 21702-5012

DISTRIBUTION STATEMENT: Approved for Public Release;
Distribution Unlimited

REPORT DOCUMENTATION PAGE

Form Approved
OMB No. 0704-0188

1. REPORT DATE
NOVEMBER 2018

2. REPORT TYPE
FINAL

3. DATES COVERED
15-AUG-2015-14-AUG-2018

4. TITLE AND SUBTITLE

Central Tolerance Blockade to Augment Checkpoint Immunotherapy in Melanoma

5a. CONTRACT NUMBER
W81XWH-15-1-0411

5b. GRANT NUMBER

5c. PROGRAM ELEMENT NUMBER

6. AUTHOR(S)

Maureen Su

E-Mail: masu@email.unc.edu

5d. PROJECT NUMBER

5e. TASK NUMBER

5f. WORK UNIT NUMBER

7. PERFORMING ORGANIZATION NAME(S) AND ADDRESS(ES)

The University of North
Carolina at Chapel Hill
104 Airport Dr., Suite 2200
CB #1350
Chapel Hill, NC 27599-1350

8. PERFORMING ORGANIZATION REPORT NUMBER

9. SPONSORING / MONITORING AGENCY NAME(S) AND ADDRESS(ES)

U.S. Army Medical Research and Materiel Command
Fort Detrick, Maryland 21702-5012

10. SPONSOR/MONITOR'S ACRONYM(S)

11. SPONSOR/MONITOR'S REPORT NUMBER(S)

12. DISTRIBUTION / AVAILABILITY STATEMENT

Approved for Public Release; Distribution Unlimited

13. SUPPLEMENTARY NOTES

14. ABSTRACT

Our preliminary data demonstrate that central tolerance blockade 1) expands the anti-melanoma immune response and 2) enhances the anti-melanoma effects of immune checkpoint inhibition. Furthermore, we have identified anti-RANKL antibody as a pharmacologic agent that blocks central tolerance. Therefore, RANKL blockade is a promising therapy for enhancing checkpoint inhibitor efficacy in advanced melanoma. This observation has immediate clinical relevance given the FDA approval of anti-RANKL antibody for other indications, including bone metastases from cancer. In order to develop anti-RANKL antibody as a combination therapy with checkpoint inhibitors for advanced melanoma patients, several critical issues remain to be clarified and are the objectives of this grant proposal. These objectives are 1) to determine whether anti-RANKL-antibody similarly depletes Aire-expressing mTECs in the human thymus and 2) to determine whether central tolerance blockade with anti-RANKL and checkpoint inhibition will have additive effects in immune rejection of melanoma in mice. Based on our preliminary data, we hypothesize that combining anti-RANKL antibody and checkpoint inhibition will have additive effects on increasing the intratumoral ratio of Teff:Treg cells and rejecting melanoma cells in mice and humans.

15. SUBJECT TERMS
Melanoma, checkpoint inhibition, anti-RANKL antibody, RANKL, anti-CTLA-4 antibody, anti-PD1 antibody, thymus, central tolerance, Aire

16. SECURITY CLASSIFICATION OF:			17. LIMITATION OF ABSTRACT	18. NUMBER OF PAGES	19a. NAME OF RESPONSIBLE PERSON
a. REPORT	**b. ABSTRACT**	**c. THIS PAGE**			USAMRMC
Unclassified	Unclassified	Unclassified	Unclassified	41	**19b. TELEPHONE NUMBER** *(include area code)*

Standard Form 298 (Rev. 8-98)
Prescribed by ANSI Std. Z39.18

TABLE OF CONTENTS

INTRODUCTION: Our preliminary data demonstrate that central tolerance blockade 1) expands the anti-melanoma immune response and 2) enhances the anti-melanoma effects of immune checkpoint inhibition. Furthermore, we have identified anti-RANKL antibody as a pharmacologic agent that blocks central tolerance. Therefore, RANKL blockade is a promising therapy for enhancing checkpoint inhibitor efficacy in advanced melanoma. This observation has immediate clinical relevance given the FDA approval of anti-RANKL antibody for other indications, including bone metastases from cancer. In order to develop anti-RANKL antibody as a combination therapy with checkpoint inhibitors for advanced melanoma patients, several critical issues remain to be clarified and are the objectives of this grant proposal. These objectives are 1) to determine whether anti-RANKL-antibody similarly depletes Aire-expressing mTECs in the <u>human</u> thymus and 2) to determine whether central tolerance blockade with anti-RANKL and checkpoint inhibition will have additive effects in immune rejection of melanoma in mice. Based on our preliminary data, **we hypothesize that combining anti-RANKL antibody and checkpoint inhibition will have additive effects on increasing the intratumoral ratio of Teff:Treg cells and rejecting melanoma cells in mice and humans.**

KEYWORDS: Melanoma, checkpoint inhibition, anti-RANKL antibody, RANKL, anti-CTLA-4 antibody, anti-PD1 antibody, thymus, central tolerance, Aire

ACCOMPLISHMENTS:

What were the major goals of the project?

Specific Aim 1. Determine whether RANKL blockade decreases mTEC cellularity in human thymus.	**Timeline**	**Site 1**
Tasks	Months	
Major Task 1. Localization of RANK and RANKL in human thymus.		
Subtask 1. Flow cytometric analysis of RANK expression in human thymus cell subsets with anti-RANK antibody.	3-6	Dr. Su, Nelson, and Markert (6 subjects)
Subtask 2. Flow cytometric analysis of RANKL expression in human thymus cell subsets with anti-RANKL antibody.	3-6	Dr. Su, Nelson, and Markert (6 subjects)
Subtask 3. Flow cytometric analysis of RANKL expression in human thymus cell subsets with OPG-Fc.	3-6	Dr. Su, Nelson and Markert (6 subjects)
Major Task 2. Effects of soluble RANKL on human mTEC cellularity.		
Subtask 1. Isolation of CD45$^-$ stromal cells from human thymus by magnetic bead separation, and verification that isolation procedure enriches for mTEC population.	6-8	Dr. Su, Nelson and Markert (3 subjects)
Subtask 2. Incubation of human CD45$^-$ thymic stromal cells with 100, 500, and 1000 ng/ml of recombinant human soluble RANKL or vehicle control. After 24 hour incubation, mTEC frequency within CD45$^-$ stromal cells will be determined by flow cytometry for each culture condition.	8-12	Dr. Su, Nelson and Markert (3 subjects)
Subtask 3. Determine relative Aire expression levels by quantitative RT-PCR in CD45$^-$ stromal cells after incubation	8-12	Dr. Su, Nelson and Markert

with 100, 500, and 1000 ng/ml of recombinant human soluble RANKL or vehicle control.		(3 subjects)
Major Task 3. Effects of in vitro blockade of RANK-RANKL interactions on human mTECs.		
Subtask 1. Culture human thymus sections with anti-RANKL antibody or isotype control at 10, 20 and 50 mcg/mL. After two week incubation, we will determine the frequency of mTECs by flow cytometry for each culture condition.	12-15	Dr. Su, Nelson and Markert (5 subjects)
Subtask 2. Culture human thymus sections with anti-RANKL antibody or isotype control at 10, 20 and 50 mcg/mL. After two week incubation, we will determine relative Aire expression by quantitative RT-PCR in cultured thymic tissue.	12-15	Dr. Su, Nelson and Markert (5 subjects)
Subtask 3. Culture human thymus sections with OPG-Fc or vehicle control. After two week incubation, we will determine the frequency of mTECs by flow cytometry for each culture condition.	15-18	Dr. Su, Nelson and Markert (5 subjects)
Subtask 4. Culture human thymus sections with OPG-Fc or vehicle control. After two week incubation, we will determine relative Aire expression by quantitative RT-PCR in cultured thymic tissue.	15-18	Dr. Su, Nelson and Markert (5 subjects)
Confirmation in adult thymus:		
Major Task 1. Localization of RANK and RANKL in human thymus.		
Subtask 1. Flow cytometric analysis of RANK expression in human thymus cell subsets with anti-RANK antibody.	21-24	Dr. Su, Moschos (2 subjects)
Subtask 2. Flow cytometric analysis of RANKL expression in human thymus cell subsets with anti-RANKL antibody.	21-24	Dr. Su, Moschos (2 subjects)
Subtask 3. Flow cytometric analysis of RANKL expression in human thymus cell subsets with OPG-Fc.	21-24	Dr. Su, Moschos (2 subjects)
Milestone(s) Achieved: Local IRB approval	20	Dr. Su
Major Task 2. Effects of soluble RANKL on human mTEC cellularity.		
Subtask 1. Isolation of CD45- stromal cells from human thymus by magnetic bead separation, and verification that isolation procedure enriches for mTEC population.	24-30	Dr. Su, Moschos (2 subjects)
Subtask 2. Incubation of human CD45- thymic stromal cells with 100, 500, and 1000 ng/ml of recombinant human soluble RANKL or vehicle control. After 24 hour incubation, mTEC frequency within CD45- stromal cells will be determined by flow cytometry for each culture condition.	24-30	Dr. Su, Moschos (2 subjects)
Subtask 3. Determine relative Aire expression levels by quantitative RT-PCR in CD45- stromal cells after incubation with 100, 500, and 1000 ng/ml of recombinant human soluble RANKL or vehicle control.	24-30	Dr. Su, Moschos (2 subjects)
Major Task 3. Effects of in vitro blockade of RANK-RANKL interactions on human mTECs.		

Subtask 1. Culture human thymus sections with anti-RANKL antibody or isotype control at 10, 20 and 50 mcg/mL. After two week incubation, we will determine the frequency of mTECs by flow cytometry for each culture condition.	30-36	Dr. Su, Moschos (2 subjects)
Subtask 2. Culture human thymus sections with anti-RANKL antibody or isotype control at 10, 20 and 50 mcg/mL. After two week incubation, we will determine relative Aire expression by quantitative RT-PCR in cultured thymic tissue.	30-36	Dr. Su, Moschos (2 subjects)
Subtask 3. Culture human thymus sections with OPG-Fc or vehicle control. After two week incubation, we will determine the frequency of mTECs by flow cytometry for each culture condition.	30-36	Dr. Su, Moschos (2 subjects)
Subtask 4. Culture human thymus sections with OPG-Fc or vehicle control. After two week incubation, we will determine relative Aire expression by quantitative RT-PCR in cultured thymic tissue.	30-36	Dr. Su, Moschos (2 subjects)
Specific Aim 2 Determine whether anti-RANKL and checkpoint inhibitors have additive effects on melanoma rejection in mice.	**Timeline**	**Site 1**
Major Task 1. Effect of concurrent anti-RANKL and checkpoint inhibitor antibody administration on intratumoral Teff:Treg ratios in melanoma-bearing mice.		
Subtask 1. Flow cytometric analysis of tumor infiltrating Teff:Treg cells in 4-8 week old C57BL/6 mice injected with B16 melanoma cells and treated with 1) anti-RANKL + isotype control 2) isotype control + anti-CTLA-4 3) anti-RANKL + anti-CTLA-4 4) isotype control + isotype control 5) isotype control + anti-CTLA-4 + anti-PD1 and 6) anti-RANKL + anti-CTLA-4 + anti-PD1.	15-24	Dr. Su, Serody (10 mice per group)
Subtask 2. Flow cytometric analysis of tumor infiltrating Teff:Treg cells in 18 month old C57BL/6 mice injected with B16 melanoma cells and treated with 1) anti-RANKL + isotype control 2) isotype control + anti-CTLA-4 3) anti-RANKL + anti-CTLA-4 4) isotype control + isotype control 5) isotype control + anti-CTLA-4 + anti-PD1 and 6) anti-RANKL + anti-CTLA-4 + anti-PD1.	24-36	Dr. Su, Serody (10 mice per group)
Subtask 3. Flow cytometric analysis of tumor infiltrating Teff:Treg cells in Tyr-CRE-ER^{T2}; Braf$^{CA/WT}$; Pten$^{F/F}$ mice treated with 1) anti-RANKL + isotype control 2) isotype control + anti-CTLA-4 3) anti-RANKL + anti-CTLA-4 4) isotype control + isotype control 5) isotype control + anti-CTLA-4 + anti-PD1 and 6) anti-RANKL + anti-CTLA-4 + anti-PD1.	15-24	Dr. Su, Serody and Sharpless (MP1U) (10 mice per group)
Subtask 4. Flow cytometric analysis of tumor infiltrating Teff:Treg cells in Tyr-CRE-ER^{T2}; LSL-Kras^{G12D}; Lkb1$^{L/L}$; P53$^{L/L}$ treated with 1) anti-RANKL + isotype control 2) isotype control + anti-CTLA-4 3) anti-RANKL + anti-CTLA-4 4)	15-24	Dr. Su, Serody and Sharpless (MP1U) (10 mice per group)

isotype control + isotype control 5) isotype control + anti-CTLA-4 + anti-PD1 and 6) anti-RANKL + anti-CTLA-4 + anti-PD1.		
Subtask 5. Flow cytometric analysis of tumor infiltrating Teff:Treg cells in C57BL/6 mice injected with B16 melanoma cells and treated with 1) anti-RANKL + isotype control 2) isotype control + anti-PD-1 3) anti-RANKL + anti-PD-1 4) isotype control + isotype control 5) isotype control + anti-CTLA-4 + anti-PD1 and 6) anti-RANKL + anti-CTLA-4 + anti-PD1.	24-36	Dr. Su, Serody (10 mice per group)
Subtask 6. Flow cytometric analysis of tumor infiltrating Teff:Treg cells in Tyr-CRE-ER^{T2}; Braf$^{CA/WT}$; Pten$^{F/F}$ mice treated with 1) anti-RANKL + isotype control 2) isotype control + anti-PD-1 3) anti-RANKL + PD-1 4) isotype control + isotype control 5) isotype control + anti-CTLA-4 + anti-PD1 and 6) anti-RANKL + anti-CTLA-4 + anti-PD1.	24-36	Dr. Su, Serody and Sharpless (MP1U) (10 mice per group)
Subtask 7. Flow cytometric analysis of tumor infiltrating Teff:Treg cells in Tyr-CRE-ER^{T2}; LSL-Kras^{G12D}; Lkb1$^{L/L}$; P53$^{L/L}$ treated with 1) anti-RANKL + isotype control 2) isotype control + anti-PD-1 3) anti-RANKL + anti-PD-1 4) isotype control + isotype control 5) isotype control + anti-CTLA-4 + anti-PD1 and 6) anti-RANKL + anti-CTLA-4 + anti-PD1.	24-36	Dr. Su, Serody and Sharpless (MP1U) (10 mice per group)
Total number of mice		420
Major Task 2. Effect of concurrent anti-RANKL and checkpoint inhibitor antibody administration on melanoma growth and host survival.		
Subtask 1. Measure tumor growth in and host survival of 4-8 week old C57BL/6 mice injected with B16 melanoma cells and treated with 1) anti-RANKL + isotype control 2) isotype control + anti-CTLA-4 3) anti-RANKL + anti-CTLA-4 4) isotype control + isotype control 5) isotype control + anti-CTLA-4 + anti-PD1 and 6) anti-RANKL + anti-CTLA-4 + anti-PD1.	13-24	Dr. Su, Serody (10 mice per group)
Subtask 2. Measure tumor growth in and host survival of 18 week old C57BL/6 mice injected with B16 melanoma cells and treated with 1) anti-RANKL + isotype control 2) isotype control + anti-CTLA-4 3) anti-RANKL + anti-CTLA-4 4) isotype control + isotype control 5) isotype control + anti-CTLA-4 + anti-PD1 and 6) anti-RANKL + anti-CTLA-4 + anti-PD1.	24-36	Dr. Su, Serody (10 mice per group)
Subtask 3. Measure tumor growth in and host survival of Tyr-CRE-ER^{T2}; Braf$^{CA/WT}$; Pten$^{F/F}$ mice treated with 1) anti-RANKL + isotype control 2) isotype control + anti-CTLA-4 3) anti-RANKL + anti-CTLA-4 4) isotype control + isotype control 5) isotype control + anti-CTLA-4 + anti-PD1 and 6) anti-RANKL + anti-CTLA-4 + anti-PD1.	13-24	Dr. Su, Serody and Sharpless (MP1U) (10 mice per group)

Subtask 4. Measure tumor growth in and host survival of Tyr-CRE-ER^{T2}; LSL-Kras^{G12D}; Lkb1$^{L/L}$; P53$^{L/L}$ treated with 1) anti-RANKL + isotype control 2) isotype control + anti-CTLA-4 3) anti-RANKL + anti-CTLA-4 4) isotype control + isotype control 5) isotype control + anti-CTLA-4 + anti-PD1 and 6) anti-RANKL + anti-CTLA-4 + anti-PD1.	13-24	Dr. Su, Serody and Sharpless (MP1U) (10 mice per group)
Subtask 5. Measure tumor growth in and host survival of C57BL/6 mice injected with B16 melanoma cells and treated with 1) anti-RANKL + isotype control 2) isotype control + anti-PD-1 3) anti-RANKL + anti-PD-1 4) isotype control + isotype control 5) isotype control + anti-CTLA-4 + anti-PD1 and 6) anti-RANKL + anti-CTLA-4 + anti-PD1.	24-36	Dr. Su, Serody (10 mice per group)
Subtask 6. Measure tumor growth in and host survival of Tyr-CRE-ER^{T2}; Braf$^{CA/WT}$; Pten$^{F/F}$ mice treated with 1) anti-RANKL + isotype control 2) isotype control + anti-PD-1 3) anti-RANKL + anti-PD-1 4) isotype control + isotype control 5) isotype control + anti-CTLA-4 + anti-PD1 and 6) anti-RANKL + anti-CTLA-4 + anti-PD1.	24-36	Dr. Su, Serody and Sharpless (MP1U) (10 mice per group)
Subtask 7. Measure tumor growth in and host survival of Tyr-CRE-ER^{T2}; LSL-Kras^{G12D}; Lkb1$^{L/L}$; P53$^{L/L}$ treated with 1) anti-RANKL + isotype control 2) isotype control + anti-PD-1 3) anti-RANKL + anti-PD-1 4) isotype control + isotype control 5) isotype control + anti-CTLA-4 + anti-PD1 and 6) anti-RANKL + anti-CTLA-4 + anti-PD1.	24-36	Dr. Su, Serody and Sharpless (MP1U) (10 mice per group)
Total number of mice		420
Milestone(s) Achieved: Local IRB Approval	13	Dr. Su

What was accomplished under these goals?

For this reporting period describe: 1) major activities; 2) specific objectives; 3) significant results or key outcomes, including major findings, developments, or conclusions (both positive and negative); and/or 4) other achievements. Include a discussion of stated goals not met. Description shall include pertinent data and graphs in sufficient detail to explain any significant results achieved. A succinct description of the methodology used shall be provided. As the project progresses to completion, the emphasis in reporting in this section should shift from reporting activities to reporting accomplishments.

As requested, we describe here progress made towards each task outlined in the entire SOW. The goal of this project is determine whether blockade of central tolerance with anti-RANKL antibody will have additive effects with checkpoint inhibitors, which act by blocking peripheral tolerance mechanisms. Data from the tasks outlined in the SOW are discussed below:

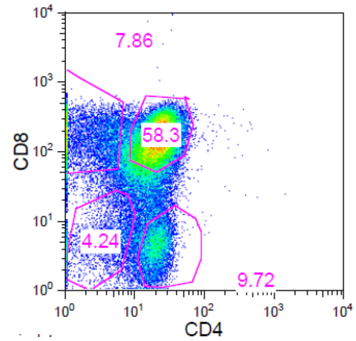

Figure 1. Representative flow cytometry plot of thymocyte subpopulations from human thymus. DP= CD4+ CD8+; DN= CD4- CD8-; CD4SP= CD4+ CD8-; CD8SP= CD4- CD8+

Specific Aim 1, Major Task 1:
We have determined the localization of RANK and RANKL in the human thymus using flow cytometry. Human thymus specimens were obtained from pediatric patients undergoing cardiac surgery. We have collaborated successfully with Dr. Jennifer Nelson, pediatric cardiac surgeon, to procure these samples immediately after removal from the patient. In total, we have collected 66 thymus samples from pediatric patients.

To address Specific Aim 1, Major Task 1, thymus specimens were minced and digested with collagenase/dispase to create a single cell suspension of human thymus cells immediately after harvesting. Cells were then stained with lineage specific markers and thymus cell subsets were detected by flow cytometry. To detect expression of RANK and RANKL on thymus cell populations, cells were stained with anti-RANKL and anti-RANK antibodies. Additionally, OPG-Fc was used as an alternative means to detect RANKL expression, since OPG is a decoy receptor for RANKL.

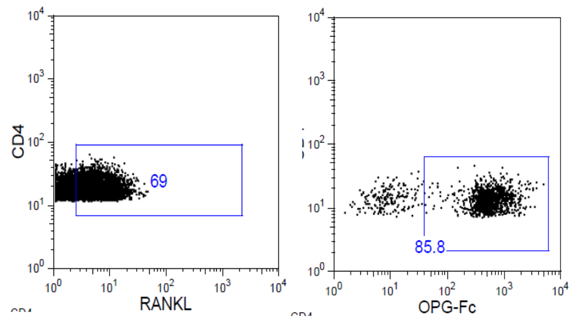

Figure 2. Representative flow cytometry plot of RANKL among CD4SP thymocyte subpopulations from human thymus. Thymocytes were stained with anti-RANKL antibody (left) or OPG-Fc (right).

As expected, four thymocyte (T cell) subpopulations (Double positive or DP; Double negative or DN; CD4+ single positive or CD4SP and CD8+ single positive or CD8SP) were delineated in the human thymus using antibodies against CD4 and CD8, as shown in Figure 1. We then used anti-RANKL antibody to detect RANKL expression. Our data indicate that RANKL is expressed by the majority of human CD4 single positive (CD4SP) cells, and by approximately 40% of CD8 single positive (CD8SP), double positive (DP), and double negative (DN) thymocytes (Figures 2 and 3, left). A higher percentage (60-80%) of these subsets are positive for RANKL expression by OPG-Fc staining (Figure 2 and 3, right). This may reflect a higher affinity of OPG-Fc for RANKL than the anti-RANKL antibody. These findings are significant because they a) recapitulate what is seen in mice, and b) suggest that RANKL is present on thymocytes and therefore can be targeted for therapy by anti-RANKL antibody.

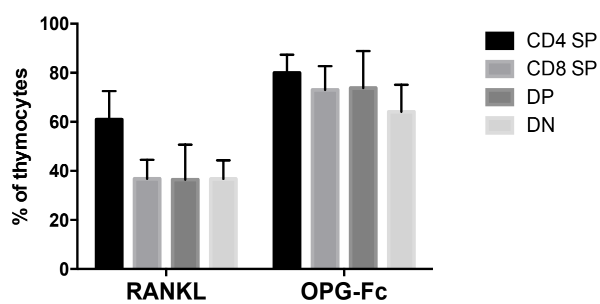

Figure 3. Average frequency of RANKL expression in the 4 subpopulations of human thymocytes. Cells were stained for RANKL using either anti-RANKL antibody (left) or OPG-Fc (right).

We have also tested for RANK expression in human thymus cell epithelial subsets (Figure 4 and 5). Human thymus cell epithelial subsets can be divided into two main subsets: medullary thymic epithelial cells (mTECs) and cortical thymic epithelial cells cTECs. mTECs can be identified by CD45-, EpCAM+, CDR2low expression, while cTECs can be identified by CD45-, EpCAM+, CDR2high expression. An example of gating strategy to identify these markers is shown in Figure 6.

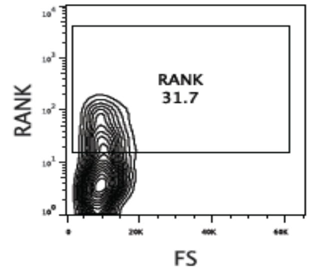

Figure 4. Representative flow cytometry plot of RANK expression in mTECs. Cells were stained with anti-RANK antibody.

Approximately 21% of CD45-, EpCAM+, CDR2low mTEC cells express RANK. In contrast, <5% of CD45-, EpCAM+, CDR2high cTECs express RANK. This is consistent with reports of RANK expression in mouse thymic epithelial cells, in which higher levels of RANK are expressed on the mTEC subset (compared to cTEC population). This suggests that blocking RANKL signaling is likely to effect mTECs without effecting cTECs, as is seen in mouse thymus.

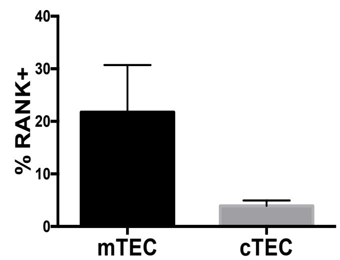

Figure 5. Average frequency of RANK expression mTECs and cTECs. Cells were stained with anti-RANK antibody.

Specific Aim 1, Major Task 2:

A key accomplishment of our project has been determining the effects of soluble RANKL on human mTEC cellularity. It has been shown by multiple groups that RANKL stimulates mTEC development and Aire expression in mice. Our goal in Specific Aim 1, Major Task 2 is to determine whether RANKL also has a similar effect in humans.

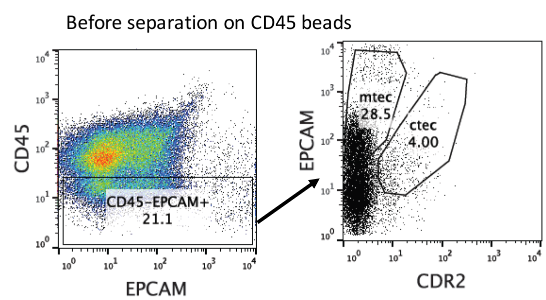

Figure 6. Human thymus cells prior to separation on CD45 magnetic beads. Flow cytometric analysis to determine fraction of CD45- cells (left), and mTEC and cTEC fractions (right).

To address this, we first determined whether isolation of CD45- stromal cells by magnetic bead separation enriches for the mTEC population. Human thymus tissue was disaggregated by mincing and collagenase/dispase digestion and made into a single cell suspension. As shown below (Figure 6), approximately 21% of cells from human thymus consist of CD45- Epcam+ cells (left). Of these CD45- Epcam+ cells, 28.5% are mTECs (right). We then enriched for CD45- cells by magnetic bead enrichment of human thymus cells. As shown below (Figure 7), of the cells in the CD45+ fraction, about 13.6% (left) were CD45- Epcam+ cells. Of the cells in the CD45- fraction, on the other hand, 89.3% of cells were CD45- Epcam+ cells (right). This represents a >6 fold enrichment in the CD45- Epcam+ fraction compared to the CD45+ Epcam+ fraction. These findings demonstrate an enrichment for CD45- Epcam+ thymic epithelial cells with Ficoll gradient centrifugation followed by magnetic bead enrichment for CD45- cells.

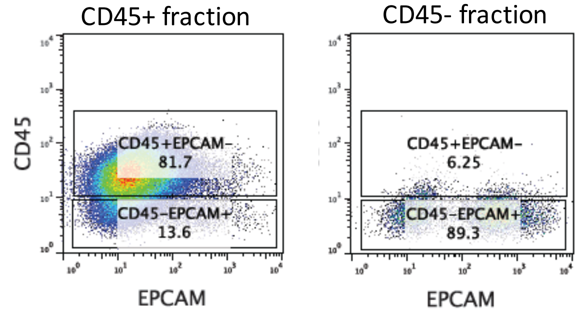

Figure 7. Increased purity of CD45- cells from human thymus after Ficoll gradient and separation with CD45 magnetic beads. Flow cytometric analysis to determine proportion of CD45- contaminants in CD45+ fraction (left) and purity of CD45- cells in CD45- fraction (right).

To further delineate the effects of magnetic bead separation, we tested whether the CD45- negative fraction was enriched for CD45- Epcam+ CDR2^{low} mTECs, we stained cells from the CD45+ (Figure 8, left) and CD45- fraction (Figure 8, right) with EPCAM and CDR2. EPCAM^{+} CDR2^{low} mTECs were enriched (~7 fold) from 9.56% to 62.2% in the CD45- fraction.

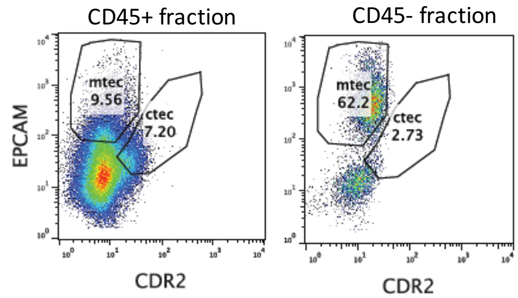

Figure 8. CD45- human thymus cells after Ficoll gradient and separation on CD45 magnetic beads are enriched for mTECs. Flow cytometric analysis to determine fraction of CD45+ cells that express mTEC markers (left), versus CD45- cells that express mTEC markers (right).

Having established that magnetic bead enrichment for CD45- cells increases the frequency of mTECs, we then sought to determine the effects of RANKL on Aire+ mTECs in culture. Enriched CD45- cells were incubated with increasing amounts of soluble human RANKL. Consistent with the hypothesis that RANK/RANKL signaling induces Aire in human mTECs, 1000 ng/mL of RANKL induced Aire expression in CD45- cells (Figure 9). We see an approximately 2 fold increase in Aire mRNA expression with 1000 ng/mL of RANKL compared to 0 and 500 ng/mL. This is an important finding because it has previously been unclear whether RANK/RANKL signaling upregulates Aire expression in human thymus.

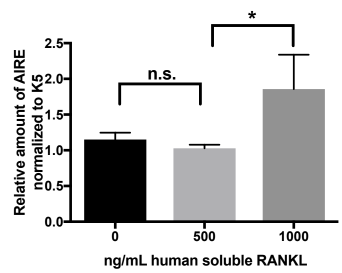

Fig. 9. Increased Aire mRNA expression with human soluble RANKL. qRT-PCR of thymus cells after incubation with human soluble RANKL at the indicated concentrations. Relative amounts were normalized to cytokeratin 5 (K5). *p<0.05 n.s.=not significant.

Specific Aim 1, Major Task 3:

Our data suggest that RANKL stimulates Aire expression in human mTECs; however, whether blocking RANK/RANKL interactions has the opposite effect on mTECs is unclear. To test this, we added aRANKL antibody to in vitro culture of human thymus cells at 3 concentrations (10, 20, and 50 mcg/mL). Surprisingly, anti-RANKL antibody at the higher concentrations (20 and 50 mcg/mL) were toxic to all cells - after 2 weeks of culture, almost all cells were dead. At 10 mcg/mL, lower cell death was noted. Thus, we performed the experiment with this concentration of anti-RANKL antibody. In paired samples that received either isotype control antibody or anti-RANKL antibody (10 mcg/mL), mTEC frequency was decreased in 5 of 6 samples tested (Figure 10). This finding suggests that RANK/RANKL interaction is important for mTEC development in humans. However, a major caveat with this experiment is the low cell viability after 2 weeks of culture.

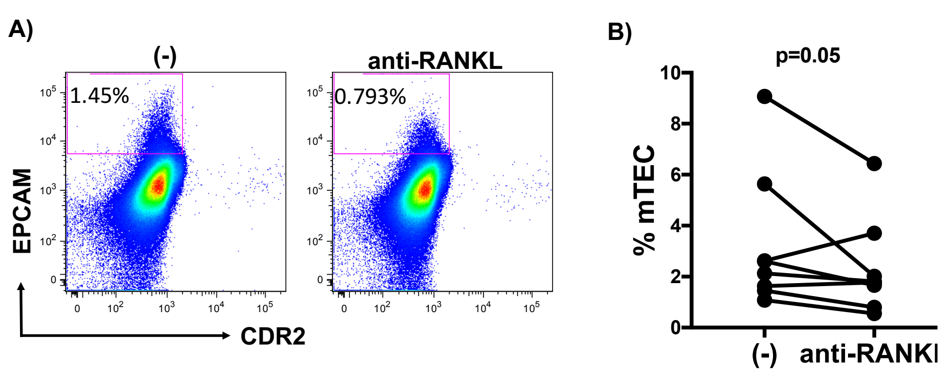

Figure 10. Decreased frequency of human mTECs after culture with anti-RANKL antibody. A) Representative flow cytometric plots of EPCAM+, CDR2- mTEC cells among CD45- cells treated with isotype control (-) or anti-RANKL antibody. B) Cumulative frequencies of mTECS with and without anti-RANKL antibody. Each dot represents an individual sample.

We next sought to determine the effects of anti-RANKL antibody (also known as denosumab) on AIRE expression in human thymus. To address this, we have performed cultures of human thymus cells with aRANKL antibody, followed by qRT-PCR for AIRE expression. We have had to modify the duration of incubation from 2 weeks, due to low cell viability and loss of Aire expression in untreated cells. Because we reasoned that we could likely detect changes in mRNA expression after 24 hours of culture, we performed qPCR for AIRE and normalized it to the housekeeping gene cytokeratin 5 (K5) at this time point. Indeed, we noted decreased Aire expression with anti-RANKL antibody (denosumab; 20 and 50 ug/mL; upper pink bars) compared to non-treated negative control (black bar). This effect was dose-dependent, since minimal effect was seen with anti-RANKL antibody (denosumab; lower pink bar) at the lowest concentration (10 ug/mL).

Figure 11. Relative Aire expression in human thymus cells with the indicated treatments. Anti-RANKL antibody (denosumab) and OPG-Fc were added for 24 hour culture.

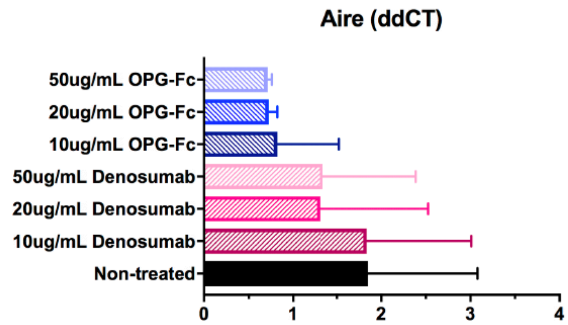

As noted above, OPG-Fc is an alternative means to block RANK/RANKL signaling, since OPG is a decoy receptor for RANKL. With OPG-Fc, decreased Aire expression was seen at all 3 concentrations tested (10, 20, and 50ug/mL). Since OPG-Fc functions to block RANK/RANKL interactions, these findings suggest that RANK/RANKL signaling is required for inducing AIRE expression, and that blocking RANK/RANKL signaling inhibits AIRE.

In sum, our data suggest that RANK is expressed on human thymocytes and RANKL is expressed on human mTECs within the thymus. Further, our data suggest that RANKL enhances Aire expression, while blocking RANK/RANKL interactions with either anti-RANKL antibody (denosumab) or OPG-Fc decreases Aire expression. In addition to the work presented here using pediatric thymi, we have also attempted to collect thymi from adult patients undergoing warm autopsy or undergoing cardiac surgery. However, none of the 3 potential adult patients had identifiable thymuses on inspection by the surgeon or physician, likely reflecting thymus involution with age and the replacement of thymus tissue with fatty tissue. Thus, we were unable to compare our findings in pediatric thymus tissue in adults. These data suggest that anti-RANKL antibody may be most effective in younger populations, in whom thymus tissue is still abundant.

Specific Aim 2, Major Task 1:

The main goal of Specific Aim 2 is to determine whether anti-RANKL antibody and checkpoint inhibitors have synergistic effects on expanding anti-tumor immunity. We first addressed this by comparing tumor infiltrating T cells using C57BL/6 mice challenged with B16 melanoma and treated with anti-RANKL antibody and/or checkpoint inhibitors. 10^5 B16 melanoma cells were injected and intratumoral T cells isolated from B16 melanoma tumors on Day 21 after inoculation. Tumors were then minced and digested into a single cell suspension, and

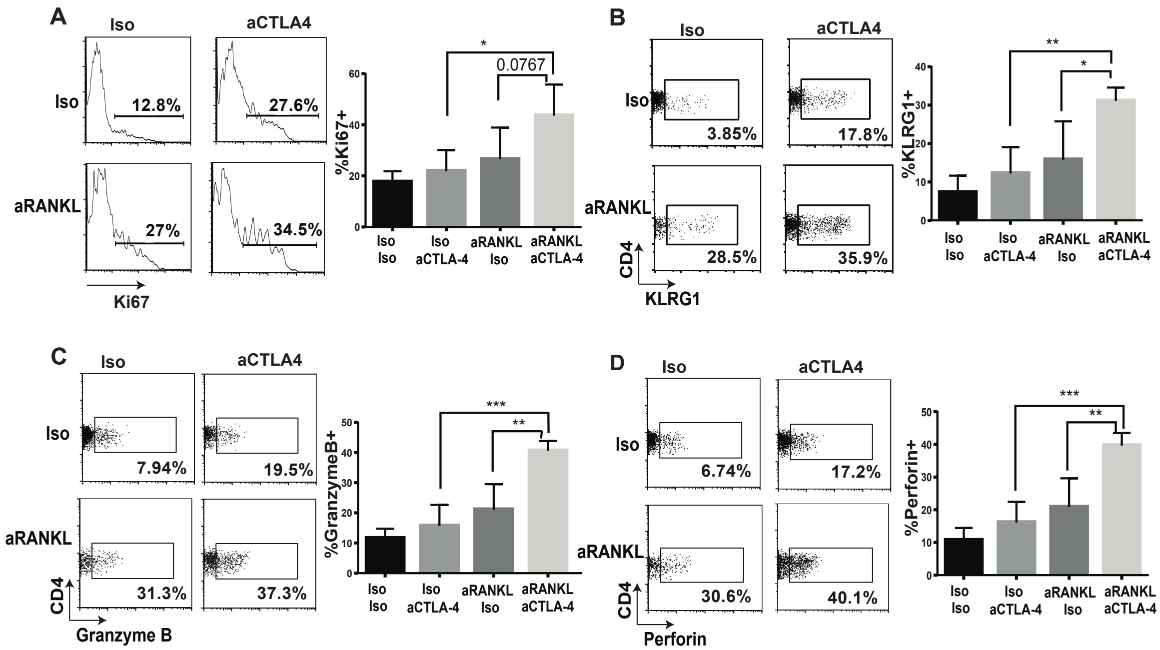

Fig. 12. Representative flow cytometry plots and average cumulative frequencies of activation markers in T cells infiltrating B16 melanoma. C57BL/6 mice were treated with isotype control (iso), anti-RANKL (aRANKL) or anti-CTLA-4 (aCTLA-4) antibodies as indicated. Flow cytometry was used to determine frequency of tumor-infiltrating CD4+ T cells that stained A) Ki67$^+$, B) KLRG1$^+$, C) Granzyme B$^+$, and D) perforin+. n=9-12 in each group, *p<0.05, **p<0.01. ***p<0001.

frequencies of tumor infiltrating T cells expressing markers of activation were delineated by flow cytometry. As noted in Figure 12 (and Figure 6C and D in Bakhru et al, *JCI Insight*), T cells from mice treated with anti-RANKL/anti-CTLA-4 (aRANKL/aCTLA-4) antibodies in combination express increased levels of A) Ki67, a marker of proliferation; B) KLRG1, a marker of activation, C) Granzyme B, a marker of cytolytic CD4+ T cells; and D) perforin, an alternative marker of cytolytic CD4+ T cells, compared to treatments with either aRANKL or aCTLA-4 antibodies as single agents. Additionally, we have published that regulatory T cell (Treg) frequencies were paradoxically higher within melanoma tumors with anti-CTLA-4 antibody treatment, compared to isotype control (Supplemental Figures 3A-F in Bakhru et al, *JCI Insight*). These findings suggest that increased T cell activation occurs in the face of elevated Treg frequencies, and that expanded anti-tumor immunity is likely due to increased T effector cell activity.

Additionally, we treated B16 melanoma tumor-bearing mice with a triple combination regimen of anti-RANKL/anti-CTLA-4/anti-PD-1 (aRANKL/aCTLA-4/aPD-1) antibodies (Fig. 13). This combination is clinically relevant, since aCTLA-4/aPD-1 antibodies in combination are currently in use in the clinic for patients with advanced melanoma. Our data indicate that intratumoral T cells isolated from mice treated with aRANKL/aCTLA-4/aPD-1antibodies in combination express higher levels of Ki67, KLRG1, and Granzyme B when compared to aCTLA-4/aPD-1 antibodies. Together, these data suggest that anti-RANKL antibodies has additive effects with checkpoint inhibitors, either aCTLA-4 antibody alone or aCTLA-4/aPD-1 antibodies in combination.

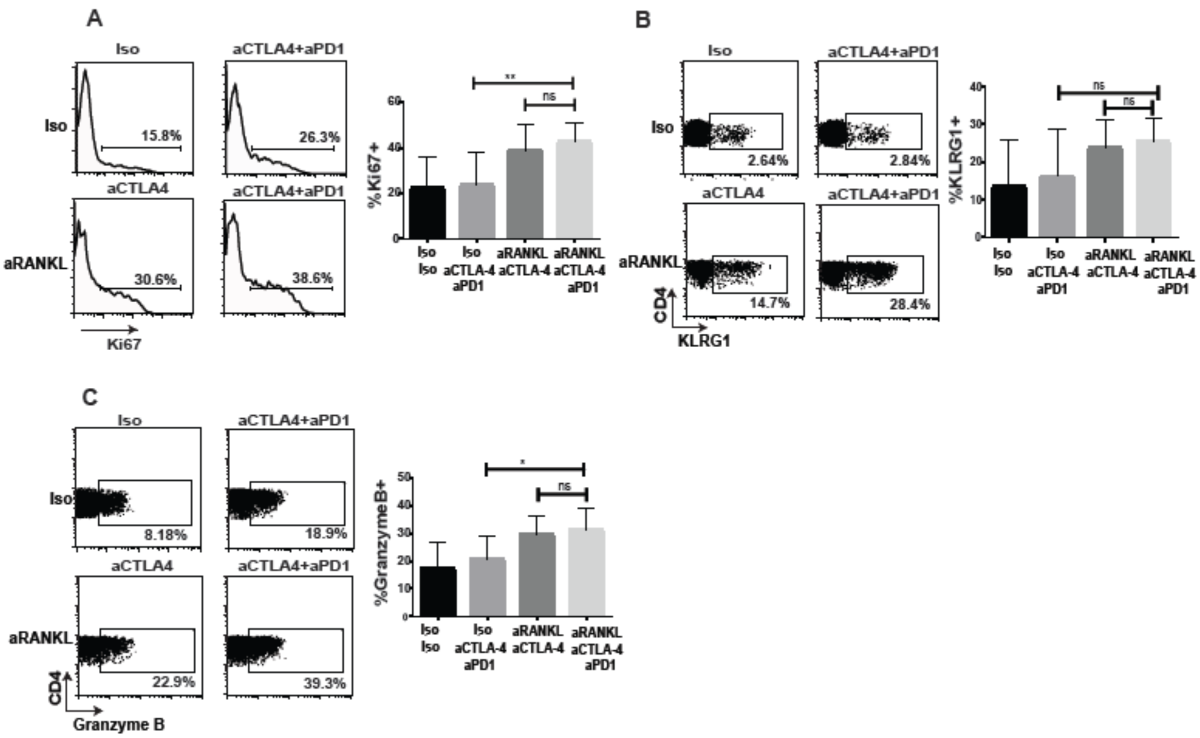

Fig. 13. Representative flow cytometry plots and average cumulative frequencies of activation markers in T cells infiltrating B16 melanoma. C57BL/6 mice were treated with anti-RANKL, anti-CTLA-4 and/or anti-PD1 antibodies as indicated. Flow cytometry was used to determine frequency of tumor-infiltrating CD4+ T cells that stained A) Ki67^{+}, B) KLRG1^{+} and C) Granzyme B^{+}. n=9-12 in each group, *p<0.05, **p<0.01. n.s.= not significant.

Interestingly, intratumoral T cells from Tyr-CRE-ER^{T2}; Braf$^{CA/WT}$; Pten$^{F/F}$ mice, a mouse model of melanoma in which melanoma develops with the topical treatment of tamoxifen on the flanks of mice, showed more variability within treatment groups. As shown in Figure 14 below, our data indicate that T cells from mice treated with anti-RANKL/CTLA-4/PD-1 antibodies in combination on average show a trend toward increased KLRG1 compared to other treatment groups (Fig. 14A). Additionally, mice treated with aRANKL/aCTLA-4 and aRANKL/aCTLA-4/aPD-1 showed a trend toward increased Ki67 expression (Figure 14B), compared to mice not receiving anti-RANKL antibody

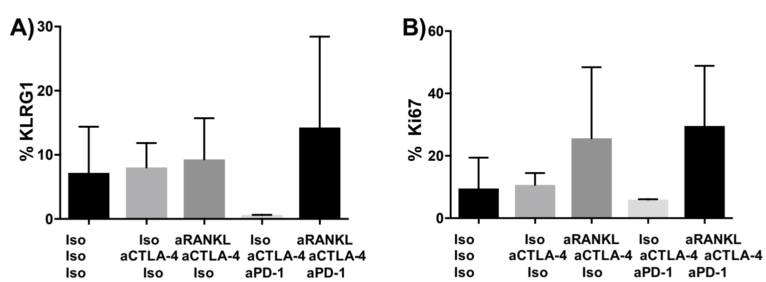

Figure 14. Average cumulative frequencies of activation markers in T cells infiltrating spontaneous melanoma. Tyr-CRE-ER^{T2}; Braf$^{CA/WT}$; Pten$^{F/F}$ mice were treated with anti-RANKL, anti-CTLA-4, and/or anti-PD-1 as indicated. A) KLRG1^{+} (left) and B) Ki67+ cells among CD4^{+} T cells was measured. n=2-6 in each group.

(iso/aCTLA-4/iso and iso/aCTLA-4/aPD-1 antibody treatments).

Specific Aim 2, Major Task 2

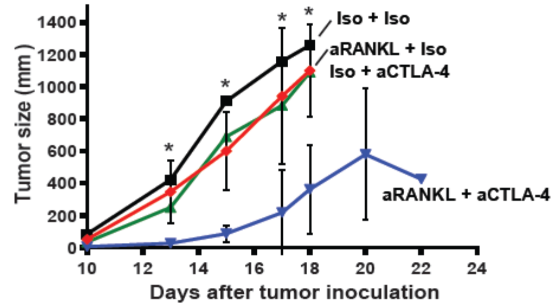

Figure 15. Tumor growth in B16 melanoma challenged mice with indicated treatments. *p<0.05 Student's t-test.

Having established increased expression of activation markers with combination aRANKL antibody and checkpoint inhibitors, we next sought to determine the effects of combination aRANKL antibody and checkpoint inhibitors on tumor growth and host survival. In the B16 melanoma model, tumor growth is decreased (Figure 15) in mice receiving both anti-RANKL and anti-CTLA-4 antibodies in combination, compared to mice receiving anti-RANKL or anti-CTLA-4 antibodies as single agents. Significant differences were noted at Day 13, 15, 17, and 18 in the size of tumors between anti-RANKL/CTLA-4 antibody treatment and either anti-RANKL antibody or anti-CTLA-4 antibody alone. Furthermore, survival of mice treated with both anti-RANKL and anti-CTLA-4 antibodies in combination was significantly improved compared to either anti-RANKL antibody or anti-CTLA-4 antibody alone (Figure 16). In line with these results, anti-RANKL antibody and anti-CTLA-4 antibodies, in the setting of GVAX (a GM-CSF expressing melanoma cell line), also has additive effects in enhancing anti-melanoma immunity. These results have been published in Bakhru et al, *JCI Insight* (Figure 6B in the paper). Together, these findings suggest that blockade of RANKL and CTLA-4 have synergistic effects in decreasing melanoma growth and increasing host survival.

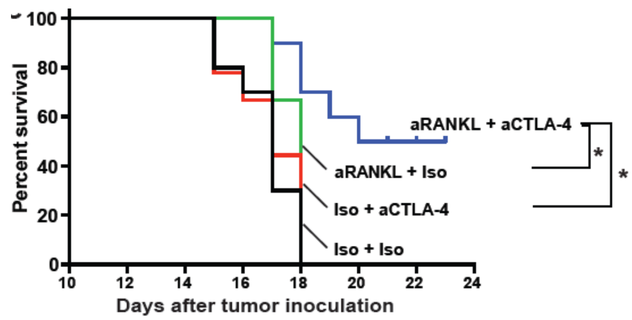

Figure 16. Survival in B16 melanoma challenged mice with indicated treatments. *p<0.05 Log-rank test.

Additionally, we treated B16 melanoma tumor-bearing mice with a triple combination regimen of anti-RANKL/anti-CTLA-4/anti-PD-1 (aRANKL/aCTLA-4/aPD-1) antibodies. As noted above, this combination is clinically relevant, since aCTLA-4/aPD-1 antibodies in combination are currently in use in the clinic for patients with advanced melanoma. Our data indicate that mice treated with aRANKL/aCTLA-4/aPD-1antibodies in combination have improved survival, compared to mice treated with combination aRANKL/aCTLA-4 and isotype control (aRANKL/aCTLA-4/iso), iso/aCTLA-4/aPD1, and iso/iso/iso control antibodies (Figure 17). These findings point to the efficacy of combining anti-RANKL with anti-CTLA-4/anti-PD-1 antibodies in improving survival in melanoma.

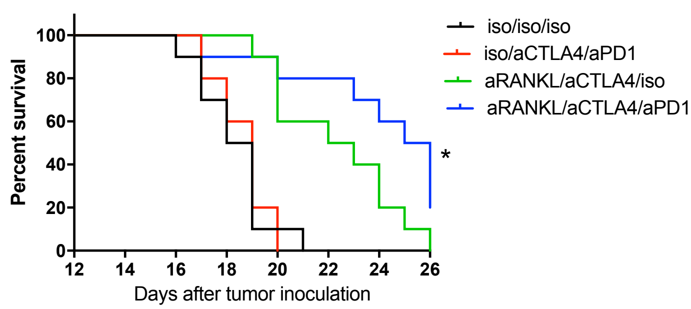

Figure 17. Survival in B16 melanoma challenged mice with indicated treatments*p<0.05 Log-rank test.

In the experiments described above, C57BL/6 mice were young adults (4-8 weeks old). Because the thymus involutes with age, and the anti-RANKL antibody appears to work via its effects on the thymus, an important question is whether aRANKL antibody therapy would still have an effect on aged mice. To address this, we treated aged mice (>18 week old, either aged in our colony or obtained from the National Institute of Aging) with anti-RANKL antibody and anti-RANKL/anti-CTLA-4 antibodies in combination. As seen in Figures 18, a delay in tumor growth was noted in mice treated with anti-RANKL antibody alone (red) compared to isotype control antibody (black). However, as seen in Figure 18, no difference was seen in percent survival with anti-RANKL antibody compared to isotype control (iso/iso). This finding suggests that anti-RANKL antibody may have some effect on tumor outgrowth, but does not increase survival. A possible reason for this could be an attenuated effect of anti-RANKL antibody in older mice. Moreover, anti-RANKL/anti-CTLA-4 antibodies in combination, when compared to aRANKL antibody alone or isotype control antibody (iso/iso), also did not decrease tumor volume or improve survival (Figures 18 and 19). This suggests that the addition of checkpoint inhibition did not further enhance anti-RANKL antibody effects in older mice. A surprising result is the accelerated growth of B16 melanoma tumors in mice treated with anti-CTLA-4 antibody alone (Figure 18, green). Whether age can also be a factor in determining the effects of checkpoint inhibition has not been explored. Although beyond the scope of this work, follow-up of this finding may be an important future direction.

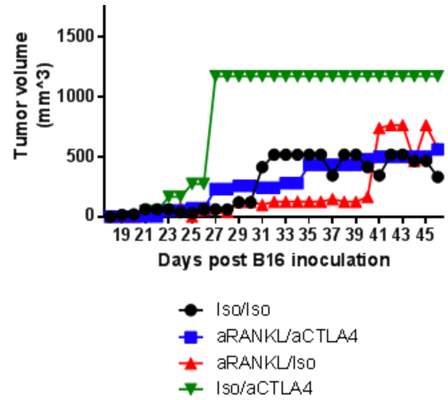

Figure 18. Tumor growth in B16 melanoma challenged aged (>18 week old) mice with indicated treatments. Iso = isotype control; aRANKL= anti-RANKL antibody; aCTLA4 = anti-CTLA4 antibody.

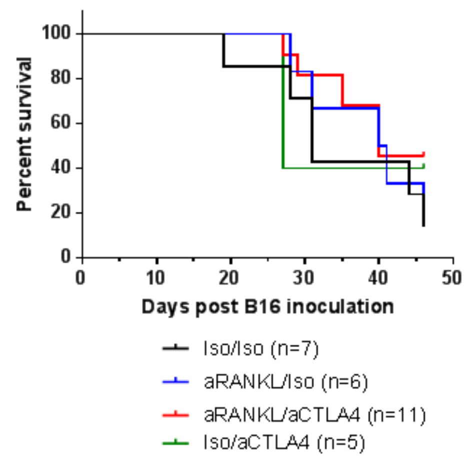

Figure 19. Survival of aged (>18 week old) mice treated with anti-RANKL (aRANKL) and/or anti-CTLA-4 (aCTLA-4) antibodies. Iso = isotype control; aRANKL= anti-RANKL antibody; aCTLA4 = anti-CTLA4 antibody.

We next explored the effects of anti-RANKL and checkpoint inhibitors in spontaneous melanoma. As described above, tumor is induced in this model with the application of tamoxifen to the flanks of Tyr-CRE-ER^{T2}; Braf$^{CA/WT}$; Pten$^{F/F}$ mice. Surprisingly, in this model, the protective effects of aRANKL antibody were not evident (Figure 20 and 21). We saw a trend toward slower tumor growth in aRANKL antibody treated (green line) and aRANKL/aCTLA4/aPD1 antibody treated (orange line) mice (Figure 20). However, the variability in tumor growth

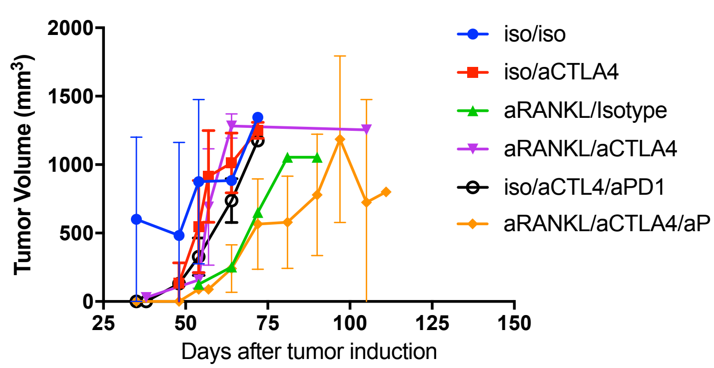

Figure 20. Tumor growth in Tyr-CRE-ER^{T2}; Braf$^{CA/WT}$; Pten$^{F/F}$ mice treated with anti-RANKL (aRANKL) and/or anti-CTLA-4 (aCTLA-4) antibodies and/or anti-PD1 (aPD1). Iso = isotype control; aRANKL= anti-RANKL antibody; aCTLA4 = anti-CTLA4 antibody.

is quite high such that statistically significant differences cannot be made. We believe this likely reflects an inherent feature of this model, and this variability in tumor growth may limit its use in treatment studies. Related to this, we have run into difficulties with breeding the second spontaneous mouse line Tyr-CRE-ER^{T2}; LSL-Kras^{G12D}; Lkb1$^{L/L}$; P53$^{L/L}$. We have been unable to obtain enough littermates of the same age to perform experiments with adequate numbers in each experimental group. However, we believe that the variability in tumor growth seen in the Tyr-CRE-ER^{T2}; Braf$^{CA/WT}$; Pten$^{F/F}$ mouse model would likely be seen in this model as well, and would also prevent us from seeing differences between group. Reflecting the high variability in tumor growth among Tyr-CRE-ER^{T2}; Braf$^{CA/WT}$; Pten$^{F/F}$ mice, no differences were seen in survival between treatment groups in this model (Figure 21). Mice treated with aRANKL/aCTLA4/aPD1 had survival similar to single treatment groups and isotype control groups. However, we believe that this is not because the treatments are not effective; instead, the lack of reproducibility in tumor growth in these models is likely obscuring any changes.

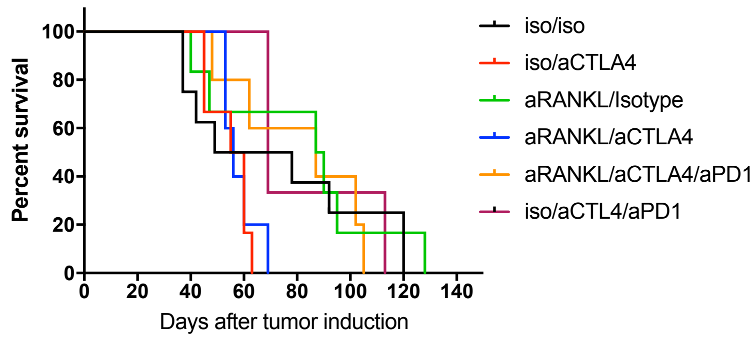

Figure 21. Survival of Tyr-CRE-ER^{T2}; Braf$^{CA/WT}$; Pten$^{F/F}$ mice treated with anti-RANKL (aRANKL) and/or anti-CTLA-4 (aCTLA-4) antibodies and/or anti-PD1 (aPD1). Iso = isotype control; aRANKL= anti-RANKL antibody; aCTLA4 = anti-CTLA4 antibody.

What opportunities for training and professional development has the project provided?

I have benefited from an active mentoring relationship with Dr. Norman Sharpless and Dr. Nancy Thomas. We met regularly to review progress and obstacles in this project. Pearl Bakhru, postdoctoral fellow in my lab, presented a poster at the UNC Postdoc Scholars Symposium and was awarded first place for her poster presentation. As stated above, this work is now published in *JCI Insight.*

How were the results disseminated to communities of interest?
As stated above, this work is now published at *JCI Insight.* We are also preparing an invited review on the topic of breaking Aire-mediated central tolerance to enhance anti-tumor immunity. This review will be published in *Cancer Immunological Research.*

What do you plan to do during the next reporting period to accomplish the goals? Not applicable, since this is a final report.

IMPACT:

What was the impact on the development of the principal discipline(s) of the project?
Based on our findings, we have initiated a Phase 2 clinical trial in human melanoma patients in which anti-RANKL antibody and checkpoint inhibitors are used in combination. If anti-RANKL antibody increases the effectiveness of checkpoint inhibitors, this could potentially have a major impact on how melanoma patients with advanced disease are treated in the clinic. These plans were directly informed by our findings from this project proposal.

What was the impact on other disciplines?

Nothing to report.

What was the impact on technology transfer?
Nothing to report.

What was the impact on society beyond science and technology?
Nothing to report.

CHANGES/PROBLEMS:
Changes in approach and reasons for change
Nothing to report.

Actual or anticipated problems or delays and actions or plans to resolve them
Nothing to report.

Changes that had a significant impact on expenditures
Nothing to report.

Significant changes in use or care of human subjects, vertebrate animals, biohazards, and/or select agents
Nothing to report.

Significant changes in use or care of human subjects
Nothing to report.

Significant changes in use or care of vertebrate animals.
Nothing to report.

Significant changes in use of biohazards and/or select agents
Nothing to report.

PRODUCTS:
- **Publications, conference papers, and presentations**

Bakhru P, Zhu ML, Wang HH, Hong LK, Khan I, Mouchess M, Gulati AS, Starmer J, Hou Y, Sailer D, Lee S, Zhao F, Kirkwood JM, Moschos S, Fong L, Anderson MS, Su MA. Combination central tolerance and peripheral checkpoint blockade unleashes antimelanoma immunity. *JCI Insight* **2,** (2017).

- **Journal publications**

Bakhru P, Zhu ML, Wang HH, Hong LK, Khan I, Mouchess M, Gulati AS, Starmer J, Hou Y, Sailer D, Lee S, Zhao F, Kirkwood JM, Moschos S, Fong L, Anderson MS, Su MA. Combination central tolerance and peripheral checkpoint blockade unleashes antimelanoma immunity. *JCI Insight* **2,** (2017).

- **Books or other non-periodical, one-time publications**
  Nothing to report.
- **Other publications, conference papers, and presentations**
  Su, MA and Anderson, MS. Controlling Aire for cancer immunotherapy. Overcoming Aire in cancer immunotherapy. *Cancer Immunological Research* invited review.
- **Website(s) or other Internet site(s)**
  Nothing to report.

- **Technologies or techniques**
  Nothing to report.
- **Inventions, patent applications, and/or licenses**
  Other Products
  Nothing to report.

PARTICIPANTS & OTHER COLLABORATING ORGANIZATIONS
What individuals have worked on the project?

Name:	Maureen Su
Project Role:	Principal Investigator
Researcher Identifier (e.g. ORCID ID):	N/A
Nearest person month worked:	4
Contribution to Project:	Maureen Su oversees this project and designs experiments.
Funding Support:	N/A
Name:	Pearl Bakhru
Project Role:	Postdoctoral Fellow
Researcher Identifier (e.g. ORCID ID):	N/A
Nearest person month worked:	6
Contribution to Project:	Pearl Bakhru performs experiments on a day to day basis.
Funding Support:	N/A
Name:	David Sailer
Project Role:	Research Assistant
Researcher Identifier (e.g. ORCID ID):	N/A
Nearest person month worked:	6
Contribution to Project:	David Sailer performs experiments on a day to day basis.
Funding Support:	N/A

Has there been a change in the active other support of the PD/PI(s) or senior/key personnel since the last reporting period?
Nothing to report.

What other organizations were involved as partners?
Nothing to report.

SPECIAL REPORTING REQUIREMENTS

- **COLLABORATIVE AWARDS:** Nothing to report.
- **QUAD CHARTS:** Nothing to report.

APPENDICES: Please see below.

JCI insight

Combination central tolerance and peripheral checkpoint blockade unleashes antimelanoma immunity

Pearl Bakhru, … , Mark S. Anderson, Maureen A. Su

JCI Insight. 2017;2(18):e93265. https://doi.org/10.1172/jci.insight.93265.

Research Article Immunology

Blockade of immune checkpoint proteins (e.g., CTLA-4, PD-1) improves overall survival in advanced melanoma; however, therapeutic benefit is limited to only a subset of patients. Because checkpoint blockade acts by "removing the brakes" on effector T cells, the efficacy of checkpoint blockade may be constrained by the limited pool of melanoma-reactive T cells in the periphery. In the thymus, autoimmune regulator (Aire) promotes deletion of T cells reactive against self-antigens that are also expressed by tumors. Thus, while protecting against autoimmunity, Aire also limits the generation of melanoma-reactive T cells. Here, we show that Aire deficiency in mice expands the pool of $CD4^+$ T cells capable of melanoma cell eradication and has additive effects with anti–CTLA-4 antibody in slowing melanoma tumor growth and increasing survival. Moreover, pharmacologic blockade of central T cell tolerance and peripheral checkpoint blockade in combination enhanced antimelanoma immunity in a synergistic manner. In melanoma patients treated with anti–CTLA-4 antibody, clinical response to therapy was associated with a human Aire polymorphism. Together, these findings suggest that Aire-mediated central tolerance constrains the efficacy of peripheral checkpoint inhibition and point to simultaneous blockade of Aire and checkpoint inhibitors as a novel strategy to enhance antimelanoma immunity.

JCI insight

Combination central tolerance and peripheral checkpoint blockade unleashes antimelanoma immunity

Pearl Bakhru,[1] Meng-Lei Zhu,[1] Hsing-Hui Wang,[1] Lee K. Hong,[1] Imran Khan,[2] Maria Mouchess,[2] Ajay S. Gulati,[1,3,4] Joshua Starmer,[5] Yafei Hou,[6] David Sailer,[1] Sandra Lee,[7,8] Fengmin Zhao,[1] John M. Kirkwood,[8,9] Stergios Moschos,[8,10,11] Lawrence Fong,[6] Mark S. Anderson,[2] and Maureen A. Su[1,11]

[1]Department of Pediatrics and Microbiology/Immunology, School of Medicine, University of North Carolina at Chapel Hill, Chapel Hill, North Carolina, USA. [2]Diabetes Center, UCSF, San Francisco, California, USA. [3]Center for Gastrointestinal Biology and Disease, [4]Department of Pathology and Laboratory Medicine, School of Medicine, and [5]Department of Genetics, University of North Carolina, Chapel Hill, North Carolina, USA. [6]Division of Hematology/Oncology, Department of Medicine, UCSF, San Francisco, California, USA. [7]Biostatistics and Computational Biology, Dana Farber Cancer Institute, Boston, Massachusetts, USA. [8]Melanoma Committee, ECOG-ACRIN Cancer Research Group, and [9]Melanoma and Skin Cancer Program, University of Pittsburgh Cancer Institute, Pittsburgh, Pennsylvania, USA. [10]Division of Hematology/Oncology, Department of Medicine, School of Medicine, and [11]Lineberger Comprehensive Cancer Center, University of North Carolina at Chapel Hill, Chapel Hill, North Carolina, USA.

Blockade of immune checkpoint proteins (e.g., CTLA-4, PD-1) improves overall survival in advanced melanoma; however, therapeutic benefit is limited to only a subset of patients. Because checkpoint blockade acts by "removing the brakes" on effector T cells, the efficacy of checkpoint blockade may be constrained by the limited pool of melanoma-reactive T cells in the periphery. In the thymus, autoimmune regulator (Aire) promotes deletion of T cells reactive against self-antigens that are also expressed by tumors. Thus, while protecting against autoimmunity, Aire also limits the generation of melanoma-reactive T cells. Here, we show that Aire deficiency in mice expands the pool of $CD4^+$ T cells capable of melanoma cell eradication and has additive effects with anti–CTLA-4 antibody in slowing melanoma tumor growth and increasing survival. Moreover, pharmacologic blockade of central T cell tolerance and peripheral checkpoint blockade in combination enhanced antimelanoma immunity in a synergistic manner. In melanoma patients treated with anti–CTLA-4 antibody, clinical response to therapy was associated with a human Aire polymorphism. Together, these findings suggest that Aire-mediated central tolerance constrains the efficacy of peripheral checkpoint inhibition and point to simultaneous blockade of Aire and checkpoint inhibitors as a novel strategy to enhance antimelanoma immunity.

Conflict of interest: The authors have declared that no conflict of interest exists.

Authorship note: PB and MLZ contributed equally to the manuscript.

Submitted: February 14, 2017
Accepted: August 10, 2017
Published: September 21, 2017

Reference information:
JCI Insight. 2017;2(18):e93265. https://doi.org/10.1172/jci.insight.93265.

Introduction

Augmenting endogenous antimelanoma T cell responses through blockade of immune checkpoints has proven effective as a therapeutic strategy against metastatic melanoma (1). Ipilimumab, a mAb targeting the coinhibitory immune checkpoint protein CTLA-4 on T cells, was the first systemic treatment to show prolonged overall survival in patients with metastatic cutaneous melanoma (2). However, anti–CTLA-4 (aCTLA-4) antibody provides disease control in only 22% of patients (2, 3), with long-term benefit in < 10% of patients (2, 4). Thus, for most metastatic melanoma patients, the antimelanoma T cell response after CTLA-4 blockade continues to be inadequate. Since the approval of ipilimumab by the FDA in 2011, two other immune checkpoint inhibitors, which target the coinhibitory immune checkpoint protein PD-1, have been approved on the basis of randomized clinical studies (5–7). Despite improved efficacy with treatments targeting PD-1, many patients still have only transient responses or do not respond to these therapies. What constrains the antimelanoma effects of checkpoint inhibitors is currently unclear (8).

Central T cell tolerance mechanisms protect against the development of autoimmunity, but also limit antitumor immunity (9–11). A key mediator of central tolerance is the Autoimmune Regulator (Aire) gene, a transcriptional activator expressed predominantly in medullary thymic epithelial cells (mTECs). There, Aire promotes expression of tissue-restricted self-antigens (TSAs) so that self-reactive thymocytes that recognize these TSAs with high affinity undergo negative selection. A subset of Aire-regulated TSAs is expressed by both melanocytes and melanoma cells. As a consequence, while purging self-reactive T cells that recognize melanocyte antigens, Aire also removes T cells capable of recognizing and eradicating melanoma cells. In humans, protection from melanoma has been associated with distinct AIRE single nucleotide polymorphisms (SNPs), which can decrease stability of Aire mRNA (12). This protection is associated with increased frequency of T cell clones recognizing MAGE-1, a self/melanoma antigen expressed in the thymus. Together, these findings support a model in which Aire deficiency prevents deletion of T cell clones that recognize self/melanoma antigens to promote a more robust T cell–mediated antitumor response.

While Aire limits antimelanoma immunity through its function in the thymus, CTLA-4 and other checkpoint proteins limit T cell responses through their activity in the immunologic periphery (13). Upon T cell receptor (TCR) activation, T cells upregulate checkpoint proteins that attenuate the T cell response (14). CTLA-4, for example, dampens early T cell activation by inducing inhibitory downstream TCR signaling and competitive inhibition of CD28-mediated coactivation. The distinct mechanisms of actions of Aire and checkpoint proteins led us to hypothesize that blockade of central Aire-mediated tolerance may interact with blockade of peripheral checkpoint inhibition to enhance T cell–mediated antimelanoma immunity.

We report here that Aire deficiency and aCTLA-4 antibody in combination have an additive effect in diminishing melanoma outgrowth and prolonging survival in melanoma-bearing mice. A pool of melanoma-reactive, cytolytic $CD4^+$ T cells that escape thymic deletion in the setting of Aire deficiency are further activated by checkpoint inhibition in the periphery, leading to an enhanced antitumor effect. Additionally, combination therapy using pharmacologic depletion of Aire-expressing mTECs (15), and inhibition of CTLA-4, significantly prolonged survival in melanoma-bearing mice compared with either strategy alone. Finally, an Aire SNP (rs1055311) is associated with response to ipilimumab therapy in metastatic melanoma patients, as part of the E1608 clinical trial, a randomized phase 2 study of ipilimumab versus ipilimumab plus GM-CSF (16). These findings point to Aire-mediated central tolerance as a key mechanism limiting the efficacy of checkpoint inhibitors and provide preclinical evidence for combining central and peripheral tolerance blockade to expand the antitumor immune response.

Results

Aire deficiency enhances antimelanoma effects of CTLA-4 blockade in mice. A dominant Aire G228W mutation results in partial loss of Aire function (17), and mice with one copy of this mutation ($Aire^{GW/+}$ mice) have increased antimelanoma immunity (11). We used $Aire^{GW/+}$ mice to test the hypothesis that Aire deficiency and peripheral checkpoint inhibition have additive effects in increasing antimelanoma immunity. CTLA-4 is a coinhibitory immune checkpoint protein induced by T cell activation. In Aire-sufficient (WT) mice challenged with B16 melanoma, aCTLA-4 antibody administration did not alter melanoma growth or host survival (Figure 1, A and B), a finding consistent with previous reports (18, 19). In $Aire^{GW/+}$ mice, on the other hand, aCTLA-4 antibody decreased melanoma growth and improved host survival compared with isotype (iso) control (Figure 1, A and B). These results suggest that Aire deficiency and aCTLA-4 antibody administration in combination have additive effects on decreasing B16 melanoma growth and improving host survival.

Human Aire polymorphism is associated with response to aCTLA-4. We investigated whether the interaction between Aire deficiency and aCTLA-4 antibody in melanoma-bearing mice might also have relevance in melanoma patients. Monoclonal aCTLA-4 IgG1 (ipilimumab) was the first checkpoint inhibitor to obtain FDA approval for patients with advanced melanoma. However, only 10%–20% of patients respond to treatment (2, 20, 21), and the factors that determine response are unclear. Multiple Aire polymorphisms, including one that may negatively affect mRNA Aire stability (12), have been associated with protection from melanoma development. This suggested that Aire polymorphisms that disrupt Aire function may enhance antimelanoma immunity in humans. Based on our findings in mice, we sought to test whether Aire polymorphisms may be associated with response to ipilimumab.

We focused on 5 Aire polymorphisms (rs1800522, rs2075876, rs56393821, rs1800520, rs1055311) that have previously been associated with melanoma protection. Seventy-nine patients with metastatic melanoma participating in the E1608 study (16) were genotyped for these 5 Aire polymorphisms. All 79 patients included in this study were randomized to the ipilimumab-alone arm. The rs1055311 TT polymorphism, which has

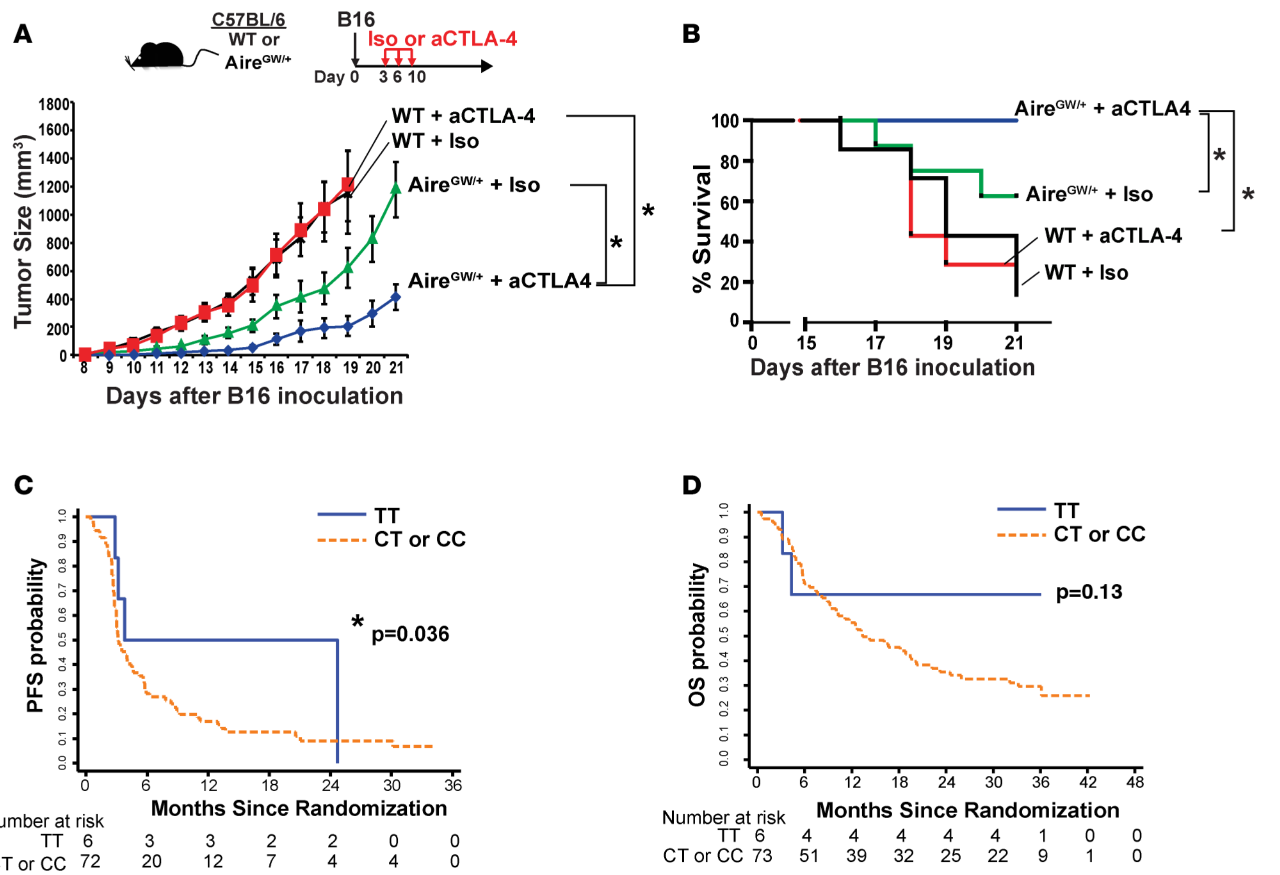

Figure 1. Association between Aire and antimelanoma effects of CTLA-4 blockade in mice and humans. (**A** and **B**) WT and *Aire*$^{GW/+}$ mice were s.c. injected with 1×10^5 B16 melanoma cells followed by anti–CTLA-4 (aCTLA-4) antibody or isotype control (iso) antibody treatment. Mice in each group were followed for B16 melanoma tumor growth and survival. n = 7–12 per group, cumulative of at least 2 independent experiments. Mann-Whitney U test. *$P < 0.05$. (**C** and **D**) Comparison of progression-free survival (PFS) and overall survival (OS) probability between patients with Aire SNP rs1055311 (TT versus CT/CC).

previously been associated with protection from melanoma development (12), was present in 6 of 79 patients (7.6%). The presence of the rs1055311 TT polymorphism was associated with increased probability of progression-free survival (Fisher's exact test, $P = 0.036$; Figure 1C) and trended toward increased probability of overall survival, although this did not reach statistical significance (log rank $P = 0.13$; Figure 1D). A caveat of these findings is the small number of patients harboring the rs1055311 TT polymorphism, which may reflect the melanoma-protective property of this SNP. These data suggest that this Aire SNP may be associated with response to ipilimumab in metastatic melanoma and should be validated in a larger-scale study.

CD4$^+$ T cells from Aire-deficient mice have increased cytolytic capacity. We next sought to delineate the cellular mechanism underlying enhanced antimelanoma immunity with combined Aire deficiency and CTLA-4 blockade. While it is known that Aire deficiency rescues melanoma-reactive CD4$^+$ and CD8$^+$ T cells from thymic deletion (10, 11), whether enhanced antitumor immunity in Aire-deficient mice is mediated by CD4$^+$ or CD8$^+$ T cells is unclear. To determine this, we purified CD4$^+$ or CD8$^+$ T cells from either *Aire*$^{GW/+}$ or WT littermates and transferred these cells into immunodeficient RAG$^{-/-}$ recipients. Recipients were then inoculated with syngeneic B16 melanoma cells. Reduced tumor growth and improved survival was associated with CD4$^+$ T cells from *Aire*$^{GW/+}$ compared with WT donors (Figure 2, A and B). In contrast, CD8$^+$ T cells from *Aire*$^{GW/+}$ and WT donors had similar effects on tumor growth and survival (Supplemental Figure 1, A and B; supplemental material available online with this article; https://doi.org/10.1172/jci.insight.93265DS1). While the absolute number of CD4$^+$ T cells was not significantly increased (Figure 2C), Aire deficiency was associated with increased expression of Ki67, a marker of proliferation, on transferred CD4$^+$ T cells (Figure 2D). Neither CD8$^+$ absolute numbers nor Ki67 expression, however, was increased with Aire deficiency (Supplemental Figure 1, C and D). These data suggest the possibility that CD4$^+$ T cells may mediate enhanced melanoma rejection in Aire deficiency.

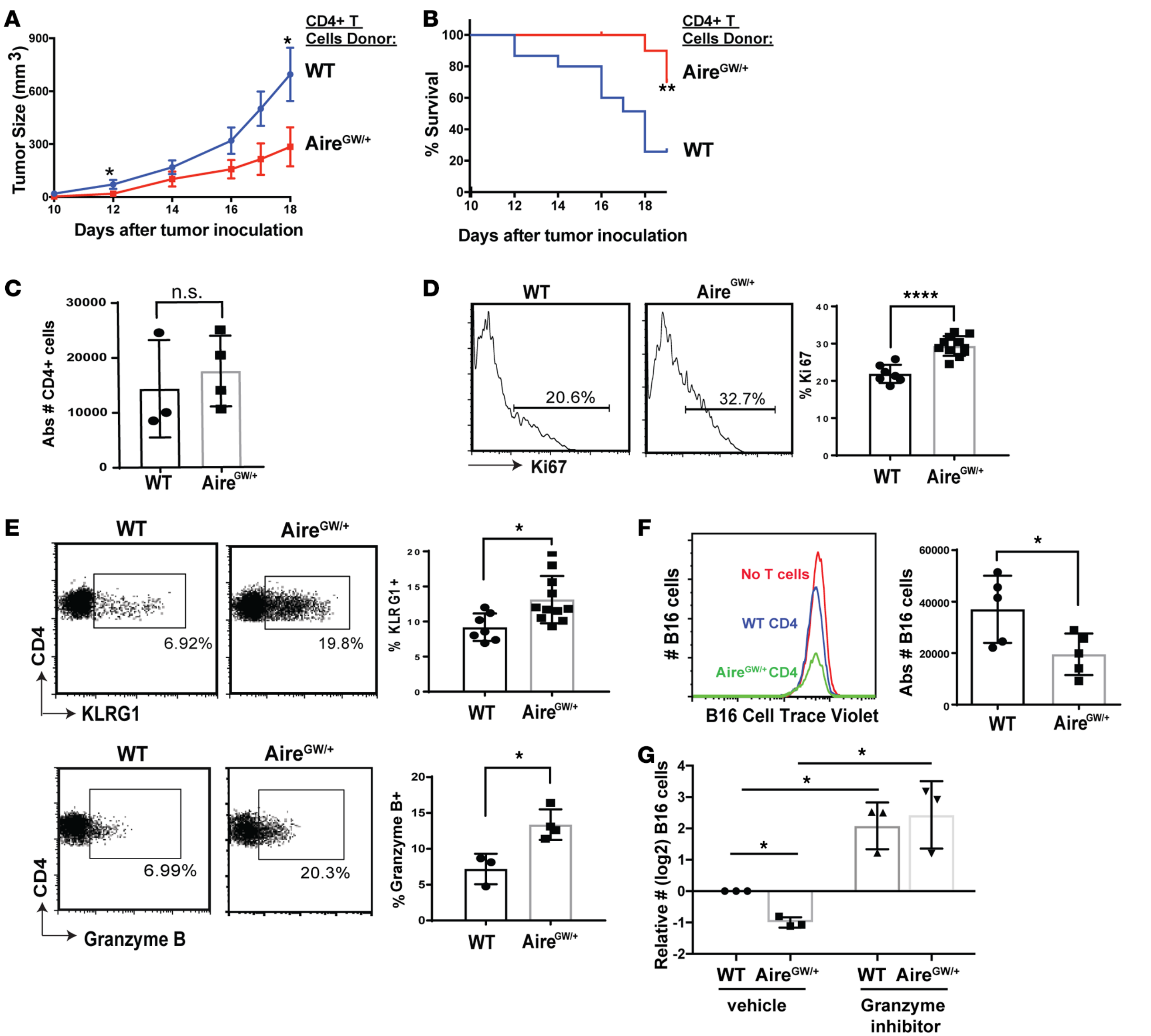

Figure 2. Aire deficiency increases CD4⁺ T cell cytolytic function to reduce melanoma growth. CD4⁺ splenocytes were transferred from WT and *Aire*$^{GW/+}$ donors into RAG$^{-/-}$ recipients, followed by s.c. B16 melanoma injection on day 7. Recipients were followed for tumor growth and survival. (**A** and **B**) B16 melanoma tumor growth and survival was measured after B16 inoculation in recipients; n = 15 per group. Mann-Whitney U test. *$P < 0.05$, **$P < 0.01$. (**C–E**) Tumor-infiltrating lymphocytes (TIL) were harvested on day 19 following B16 melanoma inoculation in recipients of either WT or *Aire*$^{GW/+}$ CD4⁺ splenocytes. Absolute numbers of CD4 tumor-infiltrating cells are shown in **C**. Two-tailed t test. Representative flow cytometry plots and average cumulative frequencies of Ki67⁺ (**D**) and KLRG1⁺ and granzyme B⁺ (**E**), among CD4⁺ T cells. Two-tailed t test. *$P < 0.05$, ****$P < 0.0001$. (**F**) Representative flow cytometry histograms and average absolute CellTrace Violet–labeled B16 cell numbers after coincubation with WT and *Aire*$^{GW/+}$ CD4⁺ T cells. Two-tailed t test. *$P < 0.05$. (**G**) Average relative B16 cell numbers (log_2) after coincubation with CD4⁺ T cells from WT and *Aire*$^{GW/+}$ mice, along with pan-granzyme inhibitor (3, 4 Dichloroisocoumarin). One-way ANOVA and two-tailed t tests, with P values adjusted using Hommel's correction for multiple comparisons. *$P < 0.05$.

Although CD8⁺ T cells are recognized as a T cell subset capable of killing cancer cells, CD4⁺ T cells also possess direct cytolytic capacity against tumors (22, 23). In particular, CD4⁺ T cells marked by killer cell lectin–like receptor subfamily G member 1 (KLRG1) express high levels of cytotoxicity-associated genes (24). Interestingly, frequency of KLRG1⁺ tumor infiltrating lymphocytes (TILs) was increased in recipients of CD4⁺ T cells from *Aire*$^{GW/+}$ compared with WT donors (Figure 2E, top). Additionally, the frequency of TILs expressing the cytolytic protein granzyme B was increased in recipients of CD4⁺ T cells from *Aire*$^{GW/+}$ compared with WT donors (Figure 2E, bottom). To test whether Aire-deficient CD4⁺ T cells have increased cytolytic capacity, we incubated purified *Aire*$^{GW/+}$ or WT CD4⁺ splenocytes with CellTrace Violet–labeled (CTV-labeled) B16 melanoma cell targets. A greater loss of B16 cells occurred with *Aire*$^{GW/+}$ compared

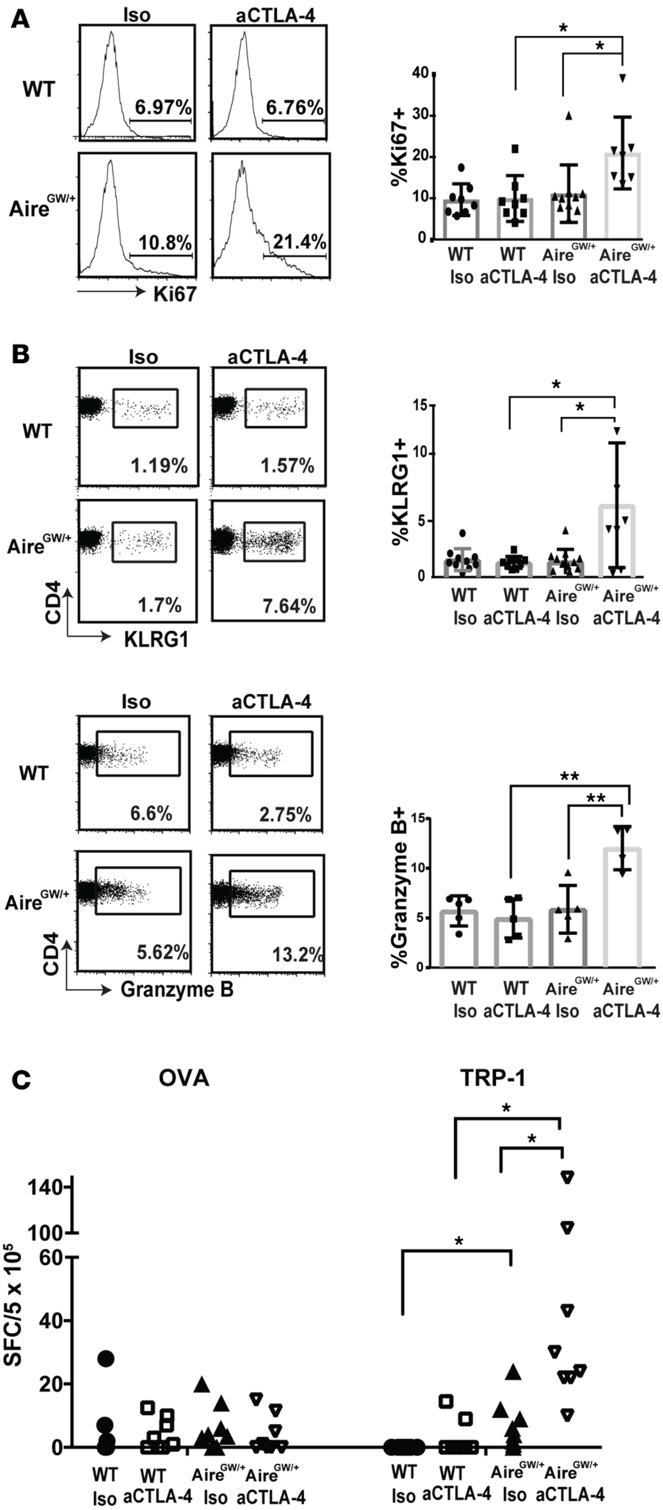

Figure 3. Additive effect of Aire deficiency and anti–CTLA-4 antibody on T cell responses. (**A** and **B**) Tumor-infiltrating lymphocytes (TIL) were harvested on day 19 following B16 melanoma inoculation in WT and *Aire*$^{GW/+}$ mice treated with aCTLA-4 or isotype control antibody (iso). Representative flow cytometry plots and average cumulative frequencies of Ki67$^+$ (**A**) and KLRG1$^+$ and granzyme B$^+$ (**B**) among CD4$^+$ T cells. n = 9–12 in each group. One-way ANOVA and two-tailed t tests with P values adjusted using Hommel's correction for multiple comparisons. *$P < 0.05$, **$P < 0.01$. (**C**) ELISPOT with splenocytes harvested on day 14 following B16 melanoma inoculation in WT and *Aire*$^{GW/+}$ mice treated with anti–CTLA-4 antibody (aCTLA-4) or iso. Cumulative spot forming cells (SFC)/5×10^5 cells secreting IL-2 with OVA and TRP-1 was analyzed. Each data point represents an individual animal. One-way ANOVA and two-tailed t tests with P values adjusted using Hommel's correction for multiple comparisons. *$P < 0.05$.

with WT CD4$^+$ T cells (Figure 2F). Similar numbers of B16 cells remained, on the other hand, after incubation with *Aire*$^{GW/+}$ and WT non-CD4$^+$ T cells (Supplemental Figure 1E). Increased B16 cytolysis by *Aire*$^{GW/+}$ CD4$^+$ T cells is mediated by granzyme, since addition of a granzyme inhibitor (3,4 dichloroisocoumarin) abrogated this effect (Figure 2G). Together, these findings suggest a critical role for cytolytic CD4$^+$ T cells in mediating the enhanced melanoma rejection associated with Aire deficiency.

Additive effect of Aire deficiency and aCTLA-4 antibody on CD4$^+$ T cell responses. We next examined the T cell response in *Aire*$^{GW/+}$ mice treated with aCTLA-4 antibody. The frequency of Ki67$^+$CD4$^+$ TILs was highest in *Aire*$^{GW/+}$ mice treated with aCTLA-4 antibody, compared with iso control–treated *Aire*$^{GW/+}$ mice or aCTLA-4 antibody–treated WT mice (Figure 3A), which suggests that Aire deficiency and aCTLA-4 antibody cooperate to increase TIL proliferation. Furthermore, frequency of CD4$^+$ T cells expressing markers associated with cytolytic activity (KLRG1, granzyme B) were also highest in *Aire*$^{GW/+}$ mice treated with aCTLA-4 antibody (Figure 3B). Among CD8$^+$ T cells, Aire deficiency and aCTLA-4 antibody did not have additive effects on increasing the frequency of Ki67$^+$ or KLRG1$^+$ cells (Supplemental Figure 2). In aCTLA-4 antibody–treated mice, Aire deficiency increased the frequency of granzyme B$^+$CD8$^+$ T cells; notably, however, in all groups, the frequency of granzyme B$^+$ cells among CD8$^+$ T cells was quite low (<2% on average). In sum, these findings suggest that Aire deficiency and CTLA-4 blockade have additive effects, primarily through activating CD4$^+$ T cells.

Interestingly, aCTLA-4 antibody administration in *Aire*$^{GW/+}$ mice increased the frequency of splenic as well as tumor-infiltrating CD4$^+$FOXP3$^+$ Tregs (Supplemental Figure 3, A–D). Furthermore, the ratio of effector-to-regulatory T cells (Teff/Treg) was similar, or lower, in Aire-deficient mice treated with aCTLA-4 antibody for both CD4$^+$CD25$^-$Teff cells and CD8$^+$ Teff cells (Supplemental Figure 3, E and F). Thus, depletion of Tregs does not underlie the additive antimelanoma effect of Aire deficiency and CTLA-4 blockade.

Aire deficiency enhances antimelanoma effects of CTLA-4 blockade in a CD4$^+$ TCR Tg mouse model. We have previously reported that the self/melanoma antigen TRP-1 is expressed in the thymus under the control of Aire (11). We therefore sought to determine whether TRP-1–specific T cells might underlie the additive antimelanoma effects of Aire deficiency and CTLA-4 blockade. To determine the antigen-specificity of activated cells, we used an IL-2 ELISPOT assay to detect rare antigen-specific T cells in the spleen of melanoma-bearing mice. As expected, Aire deficiency, with or without aCTLA-4 antibody administration, did not affect the frequency of IL-2–producing T cells reactive against the irrelevant foreign antigen OVA

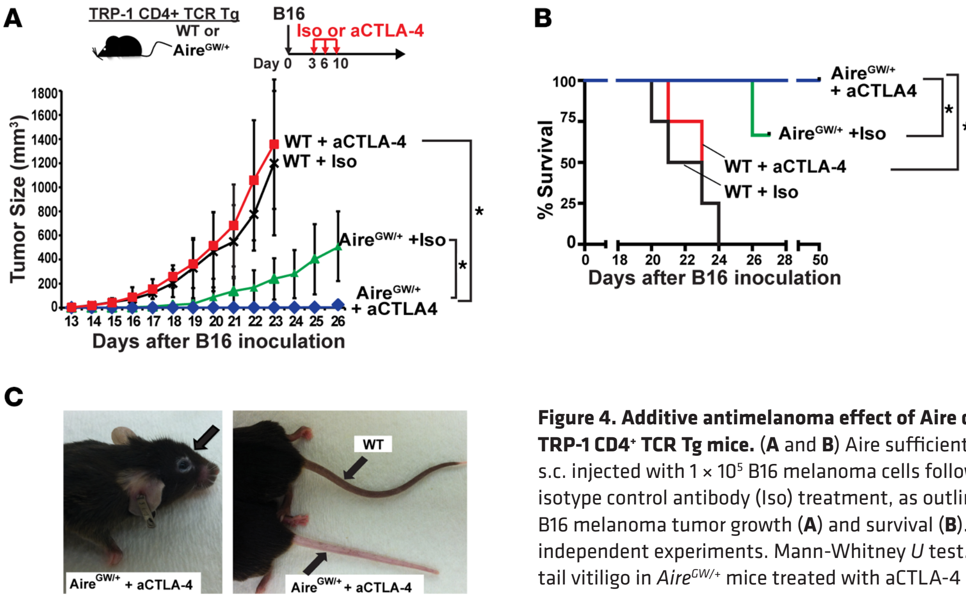

Figure 4. Additive antimelanoma effect of Aire deficiency and anti–CTLA-4 antibody in TRP-1 CD4⁺ TCR Tg mice. (**A** and **B**) Aire sufficient (WT) and *Aire*$^{GW/+}$ TRP-1 TCR Tg mice were s.c. injected with 1 × 10^5 B16 melanoma cells followed by anti–CTLA-4 antibody (aCTLA-4) or isotype control antibody (Iso) treatment, as outlined. Mice in each group were followed for B16 melanoma tumor growth (**A**) and survival (**B**). n = 7–12 per group, cumulative of at least 2 independent experiments. Mann-Whitney U test. *P < 0.05. (**C**) Examples of periporbital and tail vitiligo in *Aire*$^{GW/+}$ mice treated with aCTLA-4 antibody.

(Figure 3C, left). In contrast, Aire-deficient mice treated with iso control antibody harbored an expanded population of IL-2–producing T cells reactive against TRP-1. Moreover, aCTLA-4 antibody treatment of Aire-deficient mice further expanded the precursor frequency of IL-2–producing T cells reactive against TRP-1 (Figure 3C, right). Thus, increased melanoma rejection in *Aire*$^{GW/+}$ mice treated with aCTLA-4 antibody is accompanied by expansion of T cells recognizing TRP-1 self/melanoma antigen.

Given this finding, we used a CD4⁺ TCR Tg model to test whether CD4⁺ T cells reactive against TRP-1 may mediate the additive effects of blocking Aire and CTLA-4 in combination. TRP-1 TCR Tg mice are an MHCII-restricted mouse model in which CD4⁺ T cells recognize the melanoma antigen TRP-1 (25). In Aire sufficient (WT) TRP1-TCR Tg mice challenged with B16 melanoma, aCTLA-4 antibody administration did not affect melanoma growth or host survival (Figure 4, A and B). In *Aire*$^{GW/+}$ TRP1-TCR Tg littermates, on the other hand, aCTLA-4 antibody completely prevented tumor growth, with survival of all mice up to 50 days after tumor inoculation. These findings suggest that TRP-1–specific CD4⁺ T cells may mediate the additive antimelanoma effects of Aire deficiency and aCTLA-4 antibody administration in combination.

Vitiligo is a T cell–mediated autoimmune condition associated with effective melanoma immunotherapy (26). Notably, periorbital and tail vitiligo (Figure 4C) was observed in *Aire*$^{GW/+}$ TRP-1 TCR Tg mice treated with aCTLA-4 antibody, reminiscent of epidermal vitiligo described in ref. 27. These findings provide evidence that Aire deficiency and CTLA-4 blockade also have additive effects in autoimmune destruction of melanocytes.

aCTLA-4 antibody does not impair thymic negative selection of TRP-1 TCR Tg T cells. In our working model, we hypothesized that Aire deficiency and aCTLA-4 antibody have additive antimelanoma effects due to their function at distinct sites. Whereas Aire functions in the thymus, aCTLA-4 antibody functions in the immune periphery. However, it is possible that this model is incorrect and that aCTLA-4 may also function through altering thymocyte development. To test this possibility, we treated TRP-1 TCR Tg mice with either iso control or aCTLA-4 antibody. TRP-1 TCR Tg CD4 single positive (CD4SP) T cells undergo negative selection in an Aire-dependent manner (11) and therefore can be used to assess aCTLA-4 antibody effects. As expected, Aire deficiency results in defective negative selection, as demonstrated by the increased percent of CD4SP (%CD4SP) cells in thymi of *Aire*$^{GW/+}$ mice compared with WT (Supplemental Figure 4). In contrast, no change in %CD4SP was seen between aCTLA-4 and iso control antibody treatment in WT thymi. These findings suggest that CTLA-4 blockade does not inhibit thymic negative selection of melanoma-reactive CD4⁺ T cells. Instead, aCTLA-4 antibody may be functioning in an extrathymic manner to enhance antimelanoma immunity.

Aire deficiency does not exacerbate colitis severity in aCTLA-4 antibody–treated mice. Immune-related colitis is a frequent ipilimumab-mediated toxicity in metastatic melanoma patients and can be life-threatening (2,

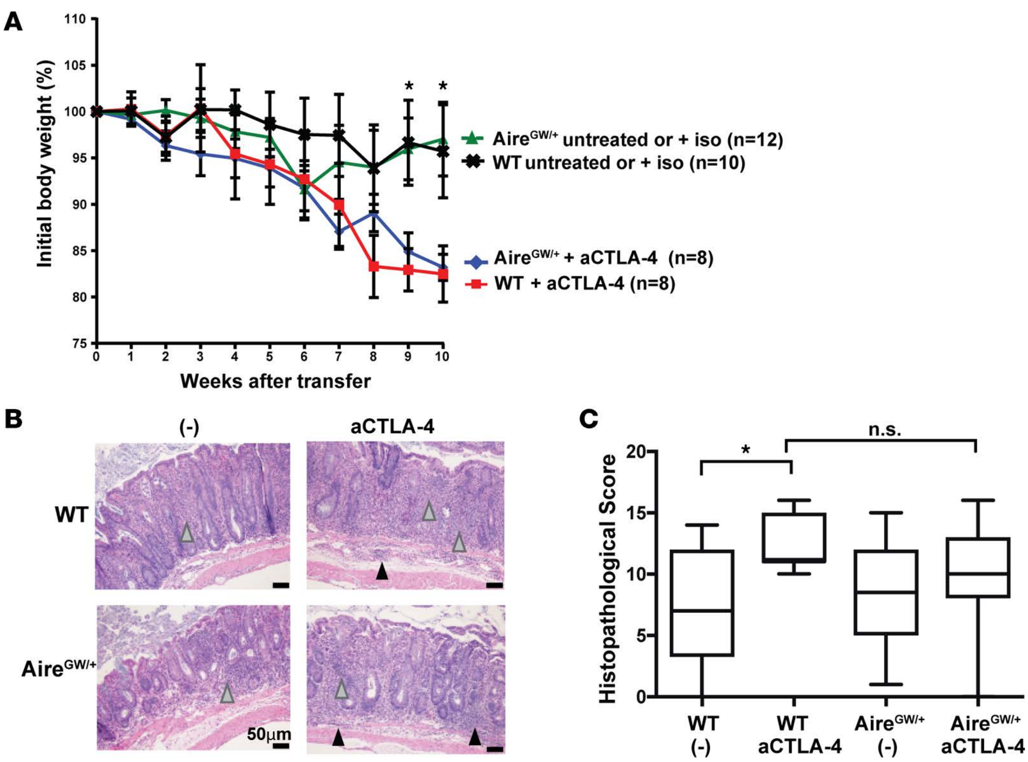

Figure 5. Aire deficiency does not exacerbate the development of experimental autoimmune colitis associated with anti–CTLA-4 antibody treatment. (**A**) Percent initial body weight of RAG$^{-/-}$ recipients after transfer of WT or *Aire*$^{GW/+}$CD4$^+$CD25$^-$CD45RB^{hi} splenocytes. After transfer, recipients were treated with anti–CTLA-4 antibody (aCTLA-4), untreated, or treated with isotype control antibody (iso). Cumulative data from 2 independent experiments are shown. *$P < 0.05$ comparing aCTLA-4 antibody treatment versus untreated/iso treatment in recipients of WT cells. (**B**) Representative H&E-stained sections of descending colons and (**C**) average histopathological scores of colons from recipients of CD4$^+$CD25$^-$CD45RB^{hi} splenocytes derived from WT and *Aire*$^{GW/+}$ mice and administered aCTLA-4 or untreated/iso (-). Gray arrowheads, immune cell infiltration in lamina propria; black arrowheads, immune cell infiltration in the submucosa. One-way ANOVA and two-tailed *t* tests with *P* values adjusted using Hommel's correction for multiple comparisons. *$P < 0.05$.

28). Likewise in mice, intestinal mucosal inflammation in experimental autoimmune colitis is exacerbated by aCTLA-4 antibody administration (29). Whether Aire deficiency promotes the colitogenic effects of CTLA-4 blockade, however, is not known. This question is of direct clinical relevance because exacerbation of immune-mediated adverse events is a potential limiting factor in combining CTLA-4 blockade with additional immune modulating therapies.

We utilized an autoimmune colitis model induced by adoptive transfer of naive T cells into RAG$^{-/-}$ recipients (30) to test the combinatorial effects of Aire deficiency and CTLA-4 blockade on colitis severity. Naive CD4$^+$ (CD25$^-$CD45RB^{hi}) Teffs from WT or *Aire*$^{GW/+}$ mice were transferred into RAG$^{-/-}$ mice, and reconstituted recipients were treated with aCTLA-4 or iso control antibody. As expected based on prior studies (29), aCTLA-4 antibody treatment of recipients reconstituted with WT cells resulted in more severe weight loss compared with no treatment or iso control antibody (Figure 5A). Consistent with this finding, aCTLA-4 antibody administration was associated with more severe colonic inflammation by histological evaluation than control treatment in recipients of WT cells (Figure 5, B and C). Importantly, weight loss and colonic inflammation was not exacerbated by Aire deficiency in donors, even if recipients were treated with aCTLA-4 antibody. Thus, in this model of immune-mediated colitis, Aire deficiency does not exacerbate the colitogenic effects of aCTLA-4 antibody treatment. This finding is consistent with previous studies reporting that Aire does not regulate development of colitogenic T cells (31, 32).

Anti-RANKL antibody enhances the immunotherapeutic effects of checkpoint inhibition in melanoma-bearing mice. mTEC survival and Aire expression are dependent on RANKL signaling so that RANKL blockade with anti-RANKL (aRANKL) antibody depletes Aire-expressing mTECs in adult mice (15). This loss of Aire$^+$ mTECS is associated with the rescue of TRP-1–specific CD4$^+$ T cells from negative selection in the thymus (Supplemental Figure 5). aRANKL antibody thus represents a pharmacologic means to induce transient Aire deficiency through Aire-expressing mTEC depletion. Since anti-tumor effects of checkpoint

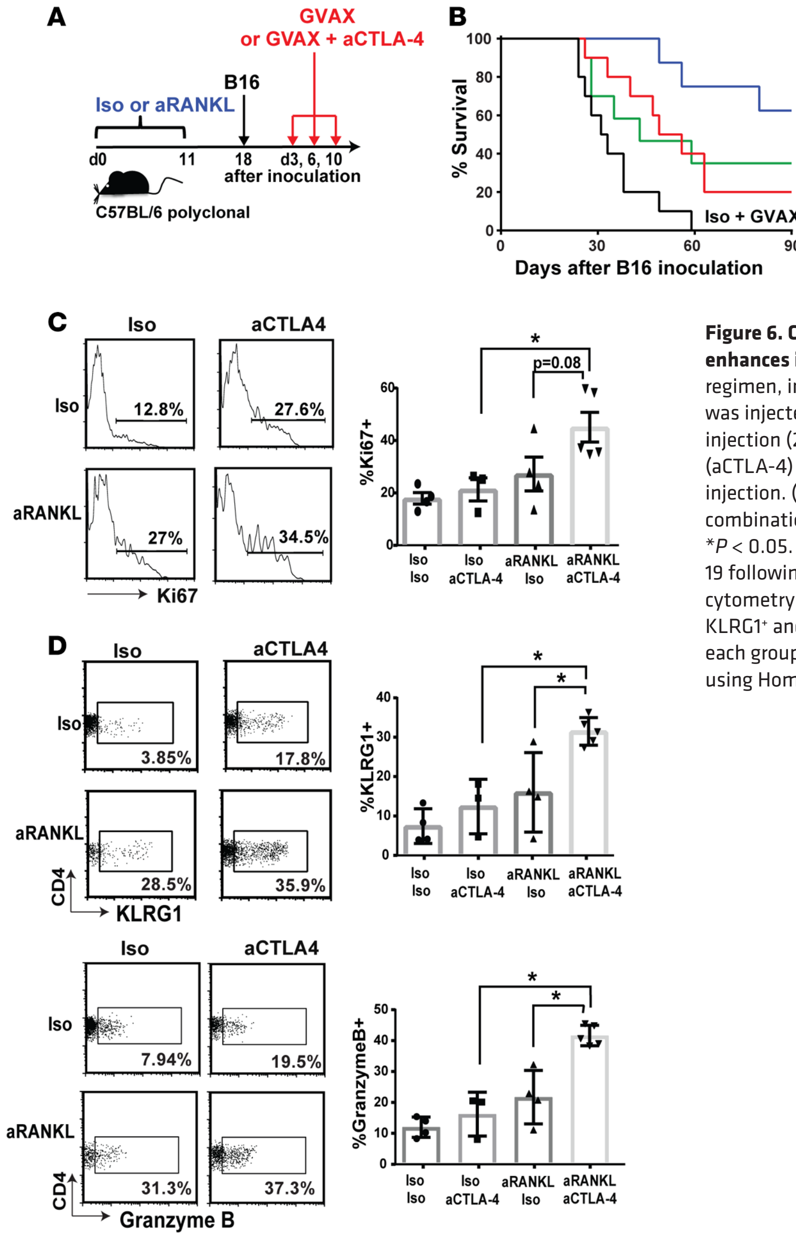

Figure 6. Combination aRANKL and aCTLA-4 antibody administration enhances immune rejection of melanoma. (**A**) Schematic of treatment regimen, in which anti-RANKL (aRANKL) or isotype control (iso) antibody was injected every other day for 11 days, followed by s.c. B16 melanoma injection (2×10^4 cells) on day 18. GVAX with or without anti-CTLA-4 (aCTLA-4) antibody was given on days 3, 6, and 10 following melanoma injection. (**B**) Survival curves in GVAX-treated mice receiving indicated combinations of therapy. n = 10 for each group. Mann-Whitney U test. *P < 0.05. Tumor-infiltrating lymphocytes (TIL) were harvested on day 19 following 1×10^5 B16 melanoma cell inoculation. Representative flow cytometry plots and average cumulative frequencies of Ki67$^+$ (**C**) and KLRG1$^+$ and granzyme B$^+$ (**D**) among CD4$^+$ T cells was measured. n = 9–12 in each group. One-way ANOVA and two-tailed t tests with P values adjusted using Hommel's correction for multiple comparisons. *P < 0.05.

inhibition could be enhanced by genetic Aire deficiency, we tested the effects of concurrent administration of aRANKL and aCTLA-4 antibodies on antimelanoma immunity. This treatment combination is clinically appealing, since aRANKL antibody is FDA approved for bone metastases, osteoporosis, and other indications, giving it a well-known safety profile (33).

Treatment with aRANKL and/or aCTLA-4 antibodies, however, did not have additive effects on improving survival in melanoma-bearing C57BL/6 polyclonal mice (data not shown). Previous studies have shown that vaccination with B16-GM-CSF (GVAX) potentiates an anti-B16 melanoma immune response through activation of innate immune cells and enhances presentation of tumor antigens to T cells (19, 34). Furthermore, addition of GM-CSF–secreting tumor vaccine to CTLA-4 blockade results in longer overall survival in patients with metastatic melanoma (16). We therefore utilized GVAX-vaccinated C57BL/6 mice to evaluate the effects of aRANKL and aCTLA-4 antibodies (Figure 6A). C57BL/6 polyclonal mice were administered aRANKL or iso control antibody and challenged with 2×10^4 B16 melanoma cells. At days 3, 6, and 10 following melanoma inoculation, mice were treated with aCTLA-4 antibody/GVAX or GVAX alone. As expected from prior reports (19), aCTLA-4 antibody/GVAX combination therapy was more effective than GVAX alone in prolonging host survival (Figure 6B). Of note, combination therapy with aRANKL/aCTLA-4 antibody/GVAX significantly improved host survival compared with iso control/aCTLA-4 antibody/GVAX therapy or aRANKL antibody/GVAX (Figure 6B). This suggests that, in the context of GVAX, aRANKL antibody and aCTLA-4 antibody have additive effects in improving host survival in response to melanoma challenge.

To assess treatment effects on $CD4^+$ T cells, we analyzed $CD4^+$ TILs in GVAX-treated mice. Mice received either aRANKL or iso control antibody, were inoculated with 1×10^5 B16 melanoma cells, and then received either aCTLA-4/GVAX or iso control/GVAX. The frequency of $Ki67^+CD4^+$ T cells was significantly higher with aRANKL/aCTLA-4/GVAX, compared with iso/aCTLA-4/GVAX therapy (Figure 6C). Additionally, the frequency of $KLRG1^+$ and granzyme B^+ $CD4^+$ T cells was increased in the aRANKL/aCTLA-4/GVAX-treated mice compared with the control groups (Figure 6D). These findings indicate that aRANKL and aCTLA-4 antibodies cooperate to increase the frequency of tumor-infiltrating $CD4^+$ T cells expressing cytolytic markers.

Discussion

We report here that genetic Aire mutations in mice and protective Aire SNPs in humans are associated with increased efficacy of aCTLA-4 antibody. Additionally, we report that pharmacologic inhibition of Aire function with aRANKL antibody is sufficient to enhance the effects of CTLA-4 checkpoint inhibition. Findings in this paper suggest a model (Supplemental Figure 6) in which Aire normally purges self/melanoma antigen–reactive $CD4^+$ T cells in the thymus, which limits the number of self/melanoma antigen–reactive $CD4^+$ T cells available for peripheral activation by checkpoint inhibition. Genetic Aire deficiency or aRANKL antibody administration allows self/melanoma-reactive T cells to escape negative selection in the thymus, and the increased pool of self/melanoma-reactive T cells available for targeting by aCTLA-4 antibody enhances the efficacy of CTLA-4 blockade in immune rejection of melanoma.

In addition to aRANKL antibody, another therapeutic approach to increasing the pool of self/melanoma-reactive T cells in the periphery is through adoptive cellular transfer of self/melanoma-reactive T cells. Indeed, ex vivo expansion and reinfusion of T cells specific for self/melanoma antigens have beneficial effects for some patients who fail conventional therapy (23, 35). Of note, recent reports have demonstrated increased efficacy of adoptive cellular transfer when combined with aCTLA-4 antibody (36, 37). These findings provide additional supportive evidence that repopulating the periphery with self/melanoma-reactive T cells enhances the effects of CTLA-4 blockade. aRANKL antibody administration provides the advantage of being a relatively straightforward therapy when compared with adoptive cellular transfer, so it may be simpler to adapt to the clinical setting. Importantly, our data demonstrate the effects of aRANKL antibody prior to B16 inoculation. The effect of aRANKL antibody on already-established tumors will be the focus of future studies.

aCTLA-4 antibody treatment has been reported to have pleiotropic effects on T cells, which include intratumoral Treg depletion and promoting increased Teff/Treg ratios (18, 22, 38, 39). Interestingly, however, Aire deficiency and CTLA-4 blockade in combination did not result in intratumoral Treg depletion in our studies. Instead, decreased melanoma growth with Aire deficiency and CTLA-4 blockade was associated with increased intratumoral $CD4^+$ T cell KLRG1 expression and cytolytic protein expression. These findings add to recent reports that $CD4^+$ T cells have direct antitumor effects, especially if clonally expanded (22, 40), and that aCTLA-4 antibody treatment activates tumor-reactive cytotoxic $CD4^+$ T cells (41).

CTLA-4 blockade is associated with colitis and other immune-related adverse events (2, 28). This finding is not surprising, since genetic deficiency of CTLA-4 in mice results in lymphoproliferation and multiple autoimmune manifestations (42, 43). Colitis can be life-threatening and is the most common ipilimumab-related toxicity in metastatic melanoma patients. Therefore, it is important to consider whether potential treatment modalities to be used in combination with CTLA-4 blockade will exacerbate colitis. We show in this study that lack of Aire function does not add to the severity of colitis in aCTLA-4 antibody–treated hosts. This result may seem unexpected, since Aire has a well-known role in preventing organ-specific autoimmune disease (44). Previous studies, however, have also reported that Aire does not regulate colitogenic T cell development (31, 32), possibly because colitogenic T cells may be directed against non–self-proteins such as colonic microbiota antigens. Thus, a combination of central tolerance blockade and checkpoint inhibition may improve a therapeutic index, compared with checkpoint inhibition alone.

aRANKL antibody represents a pharmacologic means to block central tolerance and can enhance the effects of checkpoint inhibitors in mice. In addition to its role in mTEC development, RANKL has a well-recognized role in the development, function, and survival of osteoclasts (45). For these effects, aRANKL antibody (denosumab) is FDA-approved for treatment of osteoporosis in postmenopausal women (46) and of other bone-related diseases (33). There is therefore substantial clinical experience with aRANKL antibody in patients, which should facilitate clinical testing to repurpose aRANKL antibody as an immunotherapy for the treatment of metastatic melanoma. Because the thymus involutes with age, whether thymus output can be manipulated in adults for therapeutic purpose is an open question. The median age at diagnosis of melanoma is 59 years, when thymic function is often assumed to be minimal. Multiple studies in mice and humans suggest that thymic function remains active in adults. Thymic output has been reported to continue in aged mice (47), and thymic function is measurable in adult humans up to age 76 (48). Our data that aRANKL antibody increases thymic output of TRP-1–specific T cells in adult mice (Supplemental Figure 5 and ref. 15) support the possibility that thymus function can be altered for therapeutic purpose in adults. Of note, a case report of a patient with metastatic melanoma who was concomitantly treated with aRANKL and aCTLA-4 antibodies also supports further study of this combination therapy (49).

Finally, checkpoint inhibitors have been shown to have therapeutic effects in a number of different cancers, including prostate and renal cancer (50). Thus, central tolerance blockade by aRANKL as a strategy to enhance the efficacy of checkpoint inhibition may be relevant in multiple cancer settings.

Methods

Mice. C57BL/6 $Aire^{GW/+}$ mice (17) and C57BL/6 $Aire^{GW/+}$ TRP-1 TCR Tg $RAG^{-/-}$ mice (11) were housed and bred in sterile, specific pathogen-free mouse facilities at the University of North Carolina at Chapel Hill and UCSF. C57BL/6 Aire WT littermate controls were used in all experiments. $RAG1^{-/-}$ mice were purchased from the Jackson Laboratory.

Antibodies and flow cytometry. Anti-CD4 (clone RM4-5), anti-CD3 (clone 145-2c11), anti-Ki67 (clone SolA15), anti-KLRG1 (clone 2F1), anti- granzyme B (clone NGZB), anti-FOXP3 (clone FJK-16s), and anti-CD25 (clone PC61.5) antibodies were purchased from eBioscience. Anti-CD8a (clone 5H10) antibody was purchased from Invitrogen. Intracellular staining for cytokines and FOXP3 were performed as in ref. 11. All samples were run on a Dako CyAn flow cytometer (Beckman-Coulter) and analyzed using FlowJo (TreeStar Inc.).

Isolation of TILs. TILs were isolated as previously described (11). Tumors were dissected and minced before incubation with collagenase type I/IV and DNase I. Lymphocytes were then enriched on Percoll density gradient prior to flow cytometric analysis.

B16 melanoma and antibody administration. B16-F10 is a TRP-1–expressing C57BL/6-derived spontaneous melanoma cell line originally purchased from the American Tissue Culture Condition. B16 melanoma cells were cultured as described in ref. 51. Mice were injected s.c. with 1×10^5 B16 melanoma cells as in ref. 11. Tumor measurements and survival were determined as described in ref. 15.

For immunotherapy experiments, aCTLA-4 mAb (clone 9D9; 100 μg/mouse, BioXcell) or IgG iso control antibody (clone MPC-11; 100 μg/mouse, BioXcell) were injected i.p. on days 3, 6, and 9 following B16 melanoma cell injection as described in ref. 52. For combination antibody administration experiments, aRANKL antibody (clone IKK22/5; 100 μg/mouse, BioXcell) or iso control antibody (clone 2A3; 100 μg/mouse, BioXcell) was injected every other day for a total of 6 doses. Nineteen days following treatment initiation, mice were s.c. injected with 2×10^4 B16-F10 melanoma cells for survival analysis and 1×10^5 for immune-phenotyping. On days 3, 6, and 10 following melanoma inoculations, aCTLA-4 antibody/GVAX therapy was administered as described in ref. 19.

Adoptive transfer of magnetically isolated (using Miltenyi Biotec beads) $CD4^+$ and $CD8^+$ T cells from the spleen of WT and $Aire^{GW/+}$ mice was performed in a 1:1 donor/recipient ratio into C57BL/6 $RAG^{-/-}$ recipients using a retro-orbital i.v. route of injection. After 7 days, recipients were injected s.c. with 1×10^5 B16-F10 melanoma cells. Tumor growth, survival, and development of vitiligo were monitored daily.

In vitro B16 cytotoxicity assay. Splenocytes from WT and $Aire^{GW/+}$ melanoma–bearing C57BL/6 mice were purified using CD4 beads (Miltenyi Biotec) and cultured in vitro with 5 μg/ml TRP-1 peptide at 37°C. Following overnight incubation, peptide-primed $CD4^+$ and non-$CD4^+$ T cells were harvested and used for in vitro cytotoxicity assay with B16-F10 melanoma cells. To determine in vitro killing of tumor targets, B16 cells were loaded with 0.5 mM CTV and coincubated for 12–14 hours with peptide-primed $CD4^+$ and non-$CD4^+$ cells. Proliferation of CTV B16 cells was analyzed by flow cytometry and quantified using CountBright Absolute counting beads (Thermo-Fisher Scientific). A serine protease inhibitor (3, 4 Dichloroisocoumarin, Enzo Life Sciences; 25 μM) was used for pan-granzyme inhibition.

In vitro IL-2 ELISPOT assay. ELISPOT assays for IL-2 release (BD Biosciences) were performed on splenic $CD4^+CD25^-$ Teffs from B16-F10 tumor–bearing C57BL/6 WT or *Aire*$^{GW/+}$ mice. $CD4^+CD25^-$ Teff cells were enriched by magnetic beads (Miltenyi Biotec). Cells (5×10^5) were plated for 20–22 hours on 96-well plates, which had been precoated with anti-mouse–purified IL-2 antibody overnight. Cells were left unstimulated in media (negative control) or stimulated with PMA-ionomycin (positive control). Cells were incubated in separate wells with 5 μg/ml of TRP1 (NCGTCRPGWRGAACNQKILTVR) purchased from Genemed Synthesis Inc. and OVA (ISQAVHAAHAEINEAGR) peptides purchased from InvivoGen. Culturing of the plates, washing, and counterstaining were performed according to manufacturers' instructions. Visualization and analysis of the spots were performed on the ImmunoSpot counter (Cellular Technology Ltd.). IL-2 response of stimulated cultures was calculated by subtracting the number of spot-forming colonies in the negative unstimulated control from the number of spot-forming colonies in the wells stimulated by peptides/5×10^5 cells.

SNP genotyping. Peripheral blood mononuclear cells (PBMC) collected as part of the ECOG-ACRIN Cancer Research Group study E1608 (16) were provided by the ECOG-ACRIN Central Biorepository and Pathology Facility. Following DNA extraction from PBMC, SNP genotyping assays (Applied Biosystems, TaqMan) were performed by the UNC-CH Mammalian Genotyping Core for the following SNPs of the Aire gene: rs1800522/rs1133779, rs2075876, rs56393821, rs1800520, and rs1055311. Genotyping for rs1055311 was confirmed by Sanger sequencing using two primers flanking exon 6 of the Aire gene (forward sequence: 5′-GAATGCAGGCTGTGGGAACT-3′; reverse sequence: 5′-AAGAGGGGCGTCAGCAATG-3′; product size 441 bp).

Experimental colitis. $CD4^+$ cells were enriched from WT and *Aire*$^{GW/+}$ female donor spleens using the $CD4^+$ T cell Isolation Kit II (Miltenyi Biotec) according to manufacturer instructions. Cells were labeled and sorted for $CD4^+CD25^-CD45RB^{hi}$ cells by fluorescence-activated cell sorting, as previously described (53). Cells (5×10^5) were injected i.p. into 4- to 7-week-old $RAG^{-/-}$ recipient mice. Three days after transfer, recipient mice were injected i.p. with 100 μg of iso (clone MPC-11, BioXCell) or anti-CTLA4 (clone 9D9, BioXCell) antibody at 3-day intervals. Weights were measured weekly from initial cell transfer. Lack of survival was defined as death or weight loss > 20%.

Colon histopathology. Colons were harvested at 10 weeks after adoptive transfer or earlier if weight loss of 20% was noted. Specimens were fixed in 10% formalin, sectioned (5 μm), and stained with H&E. Scoring for inflammation was performed as described (54, 55).

Statistics. R, PRISM 5.0 (GraphPad Software Inc.), and Microsoft Office Excel software (2013) were used to analyze data. Two-tailed t tests were used to compare differences between 2 groups. One-way ANOVA and two-tailed t tests with P values adjusted using Hommel's correction for multiple comparisons (56) were used to compare differences between more than 2 groups. Survival curves were compared by Mann-Whitney U test. $P < 0.05$ was considered significant.

Study approval. Study approval for human samples was obtained from the ECOG Laboratory Science & Pathology and Executive Review Committees. All animal studies were approved by the Animal Care and Use Committees at UNC-CH and UCSF.

Author contributions

PB, MLZ, HHW, LKH, IK, MM, YH, and DS performed the experiments and performed statistical analyses. PB, MLZ, and MAS wrote the paper and prepared figures. JS, SL, and FZ performed statistical analyses. ASG, JMK, SM, LF, and MSA helped design experiments and reviewed the final manuscript. MZ, MSA, and MAS formulated the concept.

Acknowledgments

This work was supported by Department of Defense Career Development Award (MAS and PB); University Cancer Research Fund (MAS and SM); ECOG-ACRIN CA180820, CA21115, CA180794, CA23318, and CA66636; the University of Pittsburgh grants CA180844 and CA39229; and NIH R01 AI097457 (MSA).

Address correspondence to: Maureen A. Su, Lineberger Comprehensive Cancer Center, 450 West Drive, Chapel Hill, North Carolina 27599, USA. Phone: 919.966.0259; Email: masu@email.unc.edu.

1. Pardoll DM. The blockade of immune checkpoints in cancer immunotherapy. *Nat Rev Cancer*. 2012;12(4):252–264.
2. Hodi FS, et al. Improved survival with ipilimumab in patients with metastatic melanoma. *N Engl J Med*. 2010;363(8):711–723.
3. Schadendorf D, et al. Pooled Analysis of Long-Term Survival Data From Phase II and Phase III Trials of Ipilimumab in Unresectable or Metastatic Melanoma. *J Clin Oncol*. 2015;33(17):1889–1894.
4. Wolchok JD, et al. Nivolumab plus ipilimumab in advanced melanoma. *N Engl J Med*. 2013;369(2):122–133.
5. Ribas A, et al. Pembrolizumab versus investigator-choice chemotherapy for ipilimumab-refractory melanoma (KEYNOTE-002): a randomised, controlled, phase 2 trial. *Lancet Oncol*. 2015;16(8):908–918.
6. McArthur GA, et al. Safety and efficacy of vemurafenib in BRAF(V600E) and BRAF(V600K) mutation-positive melanoma (BRIM-3): extended follow-up of a phase 3, randomised, open-label study. *Lancet Oncol*. 2014;15(3):323–332.
7. Weber JS, et al. Nivolumab versus chemotherapy in patients with advanced melanoma who progressed after anti-CTLA-4 treatment (CheckMate 037): a randomised, controlled, open-label, phase 3 trial. *Lancet Oncol*. 2015;16(4):375–384.
8. Mahoney KM, Rennert PD, Freeman GJ. Combination cancer immunotherapy and new immunomodulatory targets. *Nat Rev Drug Discov*. 2015;14(8):561–584.
9. Gotter J, Brors B, Hergenhahn M, Kyewski B. Medullary epithelial cells of the human thymus express a highly diverse selection of tissue-specific genes colocalized in chromosomal clusters. *J Exp Med*. 2004;199(2):155–166.
10. Träger U, et al. The immune response to melanoma is limited by thymic selection of self-antigens. *PLoS ONE*. 2012;7(4):e35005.
11. Zhu ML, Nagavalli A, Su MA. Aire deficiency promotes TRP-1-specific immune rejection of melanoma. *Cancer Res*. 2013;73(7):2104–2116.
12. Conteduca G, et al. The role of AIRE polymorphisms in melanoma. *Clin Immunol*. 2010;136(1):96–104.
13. Chambers CA, Cado D, Truong T, Allison JP. Thymocyte development is normal in CTLA-4-deficient mice. *Proc Natl Acad Sci USA*. 1997;94(17):9296–9301.
14. Page DB, Postow MA, Callahan MK, Allison JP, Wolchok JD. Immune modulation in cancer with antibodies. *Annu Rev Med*. 2014;65:185–202.
15. Khan IS, et al. Enhancement of an anti-tumor immune response by transient blockade of central T cell tolerance. *J Exp Med*. 2014;211(5):761–768.
16. Hodi FS, et al. Ipilimumab plus sargramostim vs ipilimumab alone for treatment of metastatic melanoma: a randomized clinical trial. *JAMA*. 2014;312(17):1744–1753.
17. Su MA, et al. Mechanisms of an autoimmunity syndrome in mice caused by a dominant mutation in Aire. *J Clin Invest*. 2008;118(5):1712–1726.
18. Simpson TR, et al. Fc-dependent depletion of tumor-infiltrating regulatory T cells co-defines the efficacy of anti-CTLA-4 therapy against melanoma. *J Exp Med*. 2013;210(9):1695–1710.
19. van Elsas A, Hurwitz AA, Allison JP. Combination immunotherapy of B16 melanoma using anti-cytotoxic T lymphocyte-associated antigen 4 (CTLA-4) and granulocyte/macrophage colony-stimulating factor (GM-CSF)-producing vaccines induces rejection of subcutaneous and metastatic tumors accompanied by autoimmune depigmentation. *J Exp Med*. 1999;190(3):355–366.
20. O'Day SJ, et al. Efficacy and safety of ipilimumab monotherapy in patients with pretreated advanced melanoma: a multicenter single-arm phase II study. *Ann Oncol*. 2010;21(8):1712–1717.
21. Wolchok JD, et al. Ipilimumab monotherapy in patients with pretreated advanced melanoma: a randomised, double-blind, multicentre, phase 2, dose-ranging study. *Lancet Oncol*. 2010;11(2):155–164.
22. Quezada SA, et al. Tumor-reactive CD4(+) T cells develop cytotoxic activity and eradicate large established melanoma after transfer into lymphopenic hosts. *J Exp Med*. 2010;207(3):637–650.
23. Hunder NN, et al. Treatment of metastatic melanoma with autologous CD4+ T cells against NY-ESO-1. *N Engl J Med*. 2008;358(25):2698–2703.
24. Curran MA, Kim M, Montalvo W, Al-Shamkhani A, Allison JP. Combination CTLA-4 blockade and 4-1BB activation enhances tumor rejection by increasing T-cell infiltration, proliferation, and cytokine production. *PLoS One*. 2011;6(4):e19499.
25. Muranski P, et al. Tumor-specific Th17-polarized cells eradicate large established melanoma. *Blood*. 2008;112(2):362–373.
26. Gogas H, et al. Prognostic significance of autoimmunity during treatment of melanoma with interferon. *N Engl J Med*. 2006;354(7):709–718.
27. Harris JE, Harris TH, Weninger W, Wherry EJ, Hunter CA, Turka LA. A mouse model of vitiligo with focused epidermal depigmentation requires IFN-γ for autoreactive $CD8^+$ T-cell accumulation in the skin. *J Invest Dermatol*. 2012;132(7):1869–1876.
28. Beck KE, et al. Enterocolitis in patients with cancer after antibody blockade of cytotoxic T-lymphocyte-associated antigen 4. *J Clin Oncol*. 2006;24(15):2283–2289.
29. Liu Z, et al. B7 interactions with CD28 and CTLA-4 control tolerance or induction of mucosal inflammation in chronic experimental colitis. *J Immunol*. 2001;167(3):1830–1838.
30. Powrie F, Leach MW, Mauze S, Caddle LB, Coffman RL. Phenotypically distinct subsets of CD4+ T cells induce or protect from chronic intestinal inflammation in C. B-17 scid mice. *Int Immunol*. 1993;5(11):1461–1471.
31. Anderson MS, Venanzi ES, Chen Z, Berzins SP, Benoist C, Mathis D. The cellular mechanism of Aire control of T cell tolerance. *Immunity*. 2005;23(2):227–239.
32. Török HP, Tonenchi L, Glas J, Schiemann U, Folwaczny C. No significant association between mutations in exons 6 and 8 of the autoimmune regulator (AIRE) gene and inflammatory bowel disease. *Eur J Immunogenet*. 2004;31(2):83–86.
33. Chustecka Z. Denosumab Approved for Cancer Patients with Bone Metastases. Medscape. http://www.medscape.com/viewarticle/732891. Published November 19, 2019. Accessed August 22, 2017.
34. Dranoff G, et al. Vaccination with irradiated tumor cells engineered to secrete murine granulocyte-macrophage colony-stimulating factor stimulates potent, specific, and long-lasting anti-tumor immunity. *Proc Natl Acad Sci USA*. 1993;90(8):3539–3543.
35. Chapuis AG, et al. Transferred melanoma-specific CD8+ T cells persist, mediate tumor regression, and acquire central memory phenotype. *Proc Natl Acad Sci USA*. 2012;109(12):4592–4597.
36. Chapuis AG, et al. T-Cell Therapy Using Interleukin-21-Primed Cytotoxic T-Cell Lymphocytes Combined With Cytotoxic T-Cell Lymphocyte Antigen-4 Blockade Results in Long-Term Cell Persistence and Durable Tumor Regression. *J Clin Oncol*. 2016;34(31):3787–3795.

37. Chapuis AG, et al. Combined IL-21-primed polyclonal CTL plus CTLA4 blockade controls refractory metastatic melanoma in a patient. *J Exp Med*. 2016;213(7):1133–1139.
38. Kavanagh B, et al. CTLA4 blockade expands FoxP3+ regulatory and activated effector CD4+ T cells in a dose-dependent fashion. *Blood*. 2008;112(4):1175–1183.
39. Quezada SA, Peggs KS, Curran MA, Allison JP. CTLA4 blockade and GM-CSF combination immunotherapy alters the intratumor balance of effector and regulatory T cells. *J Clin Invest*. 2006;116(7):1935–1945.
40. Malandro N, et al. Clonal Abundance of Tumor-Specific CD4(+) T Cells Potentiates Efficacy and Alters Susceptibility to Exhaustion. *Immunity*. 2016;44(1):179–193.
41. Kitano S, et al. Enhancement of tumor-reactive cytotoxic CD4+ T cell responses after ipilimumab treatment in four advanced melanoma patients. *Cancer Immunol Res*. 2013;1(4):235–244.
42. Tivol EA, Borriello F, Schweitzer AN, Lynch WP, Bluestone JA, Sharpe AH. Loss of CTLA-4 leads to massive lymphoproliferation and fatal multiorgan tissue destruction, revealing a critical negative regulatory role of CTLA-4. *Immunity*. 1995;3(5):541–547.
43. Waterhouse P, et al. Lymphoproliferative disorders with early lethality in mice deficient in Ctla-4. *Science*. 1995;270(5238):985–988.
44. Nagamine K, et al. Positional cloning of the APECED gene. *Nat Genet*. 1997;17(4):393–398.
45. Xing L, Schwarz EM, Boyce BF. Osteoclast precursors, RANKL/RANK, and immunology. *Immunol Rev*. 2005;208:19–29.
46. Cummings SR, et al. Denosumab for prevention of fractures in postmenopausal women with osteoporosis. *N Engl J Med*. 2009;361(8):756–765.
47. Hale JS, Boursalian TE, Turk GL, Fink PJ. Thymic output in aged mice. *Proc Natl Acad Sci USA*. 2006;103(22):8447–8452.
48. Poulin JF, et al. Direct evidence for thymic function in adult humans. *J Exp Med*. 1999;190(4):479–486.
49. Smyth MJ, Yagita H, McArthur GA. Combination Anti-CTLA-4 and Anti-RANKL in Metastatic Melanoma. *J Clin Oncol*. 2016;34(12):e104–e106.
50. Egen JG, Kuhns MS, Allison JP. CTLA-4: new insights into its biological function and use in tumor immunotherapy. *Nat Immunol*. 2002;3(7):611–618.
51. Kruczynski A, Hill BT. Classic in vivo cancer models: three examples of mouse models used in experimental therapeutics. *Curr Protoc Pharmacol*. 2002;Chapter 5:Unit5.24.
52. Curran MA, Montalvo W, Yagita H, Allison JP. PD-1 and CTLA-4 combination blockade expands infiltrating T cells and reduces regulatory T and myeloid cells within B16 melanoma tumors. *Proc Natl Acad Sci USA*. 2010;107(9):4275–4280.
53. Ostanin DV, et al. T cell-induced inflammation of the small and large intestine in immunodeficient mice. *Am J Physiol Gastrointest Liver Physiol*. 2006;290(1):G109–G119.
54. Ostanin DV, et al. T cell transfer model of chronic colitis: concepts, considerations, and tricks of the trade. *Am J Physiol Gastrointest Liver Physiol*. 2009;296(2):G135–G146.
55. Read S, Powrie F. Induction of inflammatory bowel disease in immunodeficient mice by depletion of regulatory T cells. *Curr Protoc Immunol*. 2001;Chapter 15:Unit 15.13.
56. Hommel G. A Stagewise Rejective Multiple Test Procedure Based on a Modified Bonferroni Test. *Biometrika*. 1988;75:383–386.

Supplementary Figures

Supplementary Figure 1

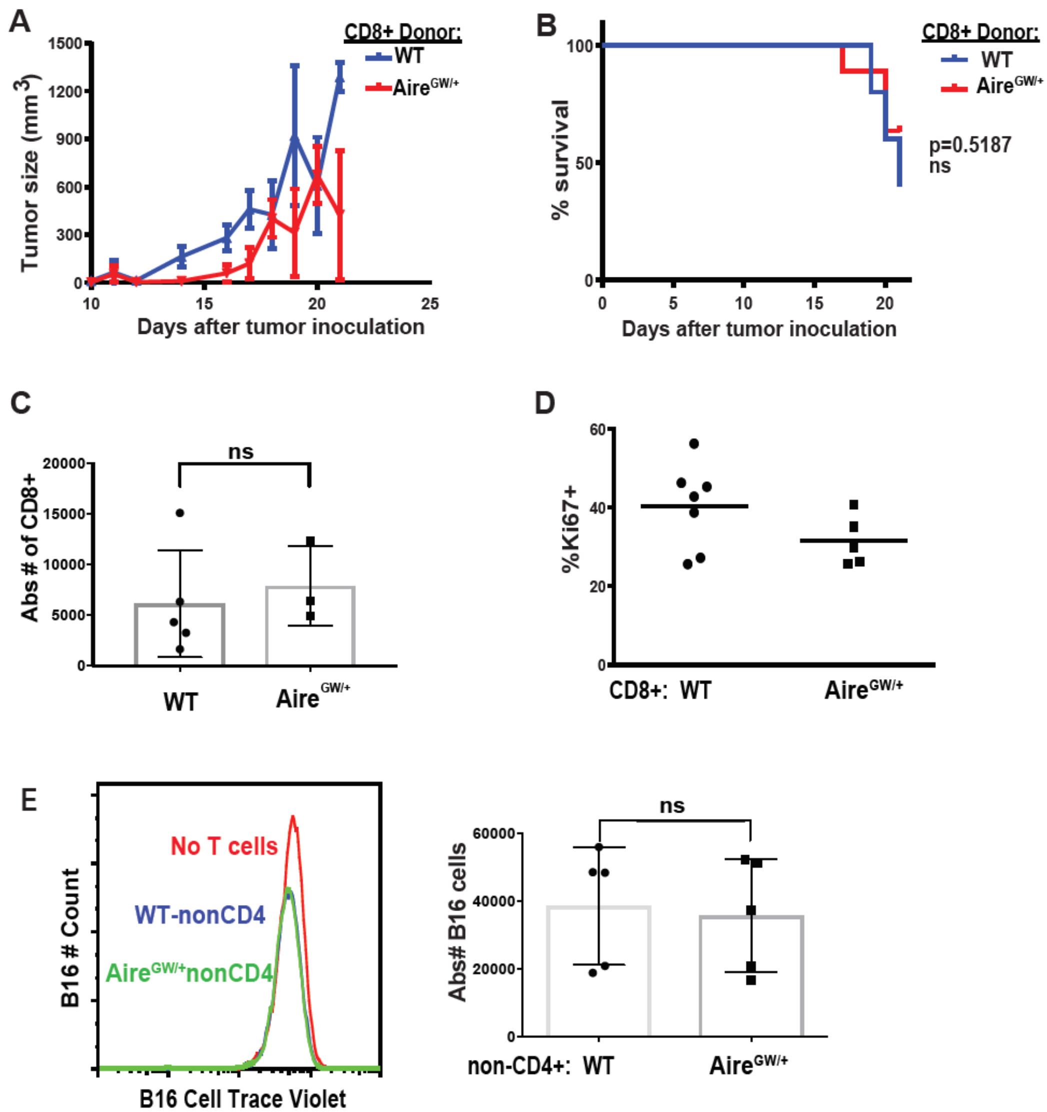

Supplementary Figure 1: Aire deficiency has minimal effects on CD8^{+} T cell cytolytic function in melanoma bearing mice. A and B) RAG$^{-/-}$ recipients of CD8^{+} T cells from WT and Aire$^{GW/+}$ mice were followed for B16 melanoma tumor growth and survival after B16 inoculation; n=10 per group, Mann Whitney U-test. *p<0.05, n.s.=non-significant. C) Absolute numbers of CD8+ tumor-infiltrating cells. t-test. ns=not significant. D) Average cumulative frequencies of Ki67^{+}

among $CD8^+$ T cells. Tumor-infiltrating lymphocytes (TIL) were harvested on Day 19 following B16 melanoma inoculation in $RAG^{-/-}$ recipients of $CD8^+$ T cells from WT and $Aire^{GW/+}$ donor mice. t-test. ns=not significant. E) Representative flow cytometry histogram comparison and average absolute B16 cell numbers of cell trace violet-labeled B16 cells after co-incubation with non-$CD4^+$ T cells from WT and $Aire^{GW/+}$ mice. t-test. ns=not significant.

Supplementary Figure 2

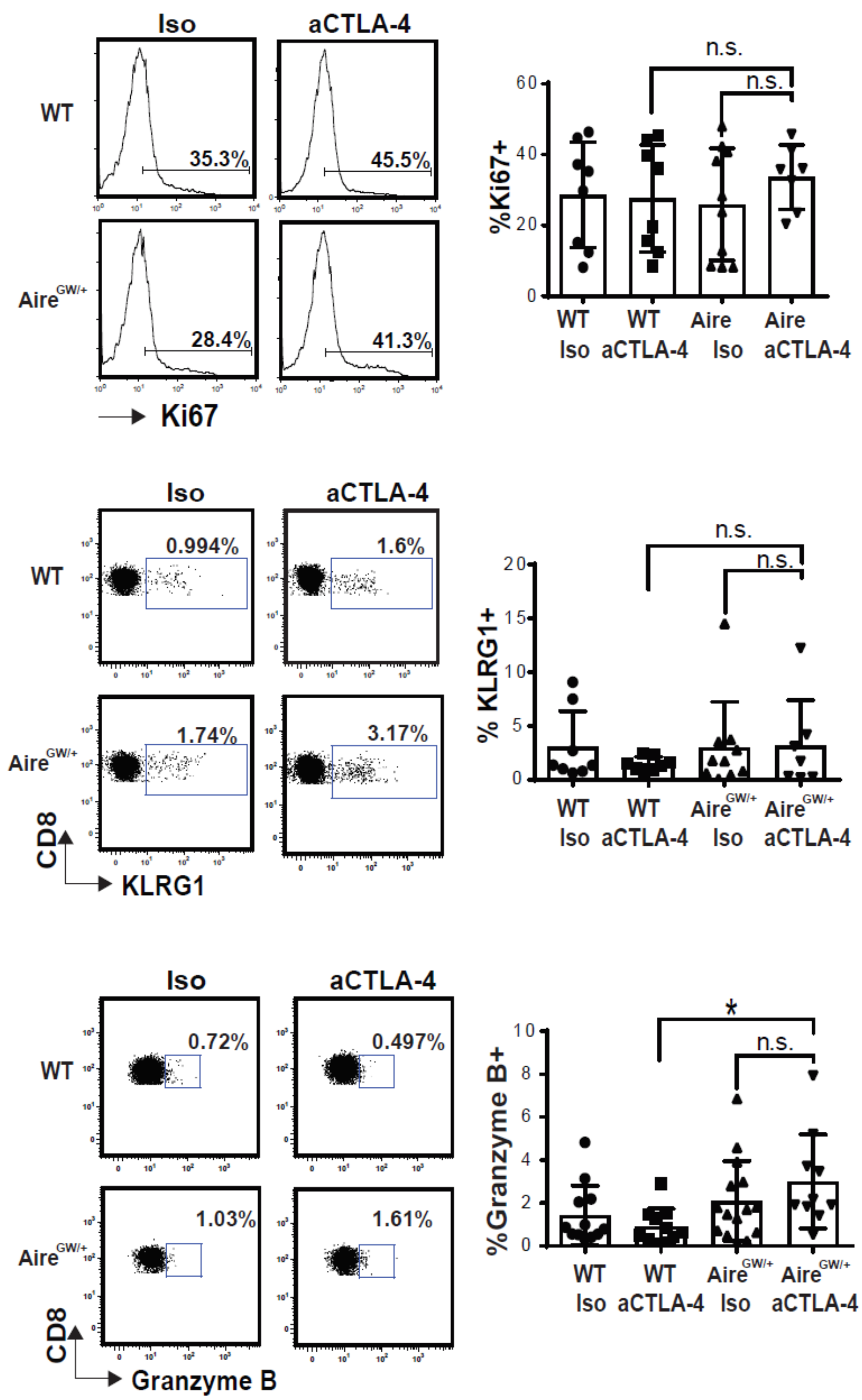

Supplementary Figure 2: Modest effect of Aire deficiency and anti-CTLA-4 antibody on CD8+ T cell responses. Tumor-infiltrating lymphocytes (TIL) were harvested on Day 19 following B16 melanoma inoculation in WT and $Aire^{GW/+}$ mice treated with aCTLA-4 or iso antibody. Representative flow cytometry plots and average cumulative frequencies of $Ki67^{+}$, $KLRG1^{+,}$ and Granzyme B^{+} among $CD8^{+}$ T cells. n=9-12 in each group. One-way ANOVA with Tukey's multiple comparisons test. ns=not significant, *p<0.05.

Supplementary Figure 3

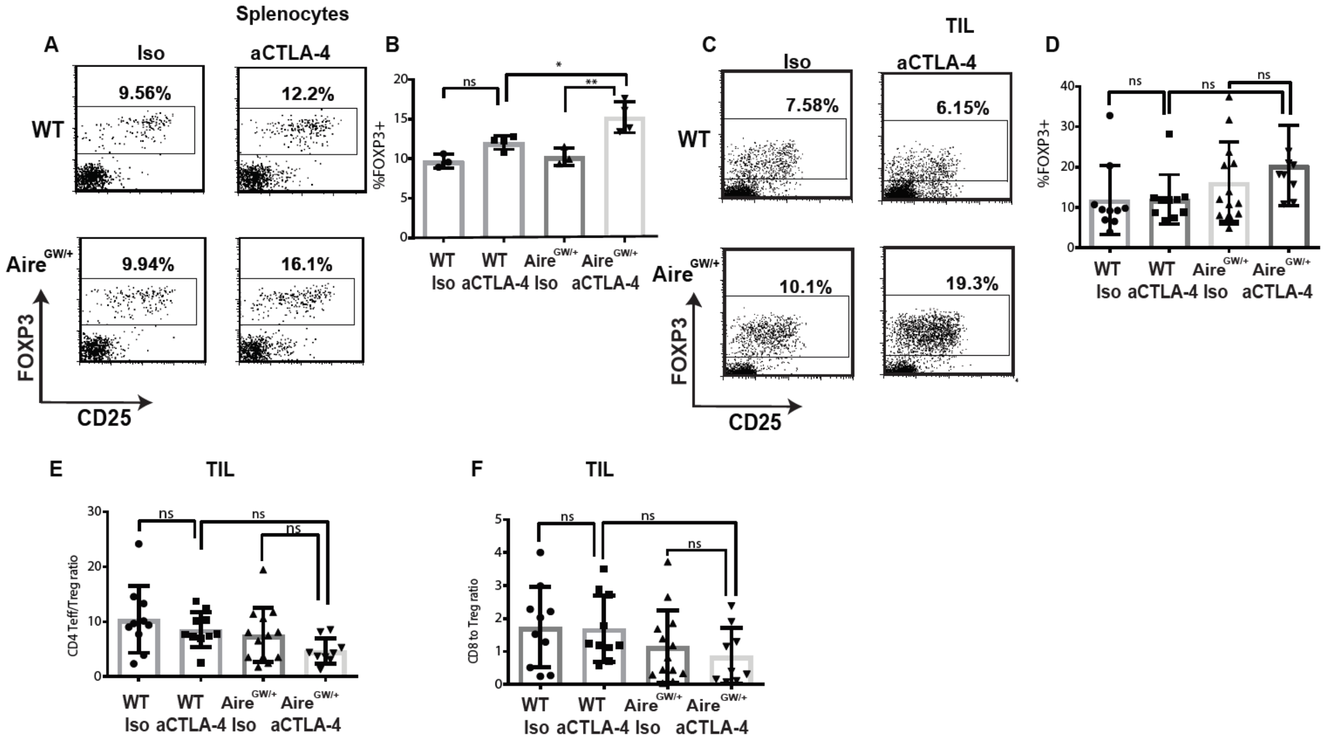

Supplementary Figure 3: Anti-CTLA-4 antibody treatment in Aire deficient mice does not decrease Treg population. Splenocytes and tumor-infiltrating lymphocytes (TIL) were harvested on Day 19 following B16 melanoma inoculation in WT and Aire$^{GW/+}$ mice treated with anti-CTLA-4 antibody (aCTLA-4) or isotype control antibody (Iso). A) Representative flow cytometry plots of FOXP3 and CD25 expression and (B) average cumulative frequencies of FOXP3^{+} Tregs within CD4^{+} splenocyte population. C) Representative flow cytometry plots of FOXP3 and CD25 expression and (D) average cumulative frequencies of FOXP3^{+} Tregs within CD4^{+} TIL population. E and F) Average cumulative ratio of CD4^{+} Teffs : FOXP3^{+} Tregs (E) and CD8^{+} T cells : FOXP3^{+} Tregs (F). One-way ANOVA with Tukey's multiple comparisons test. *p<0.05, **p<0.01, n.s= not significant.

Supplementary Figure 4

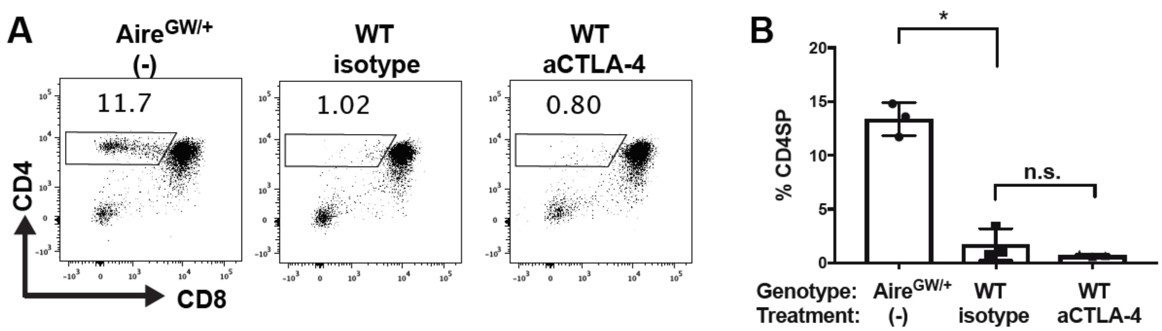

Supplementary Figure 4: anti-CTLA-4 antibody does not impair negative selection of TRP-1 specific CD4+ T cells. A) Representative flow cytometric plots of CD4+ and CD8+ thymocytes from Aire$^{GW/+}$ or WT TRP-1 TCR Tg mice. WT TRP-1 TCR Tg were treated with either isotype control antibody (iso) or anti-CTLA-4 antibody (aCTLA-4). B) Cumulative frequency (mean +/- SD) of CD4 single positive (SP) cells. One-way ANOVA with Tukey's multiple comparisons test. *p<.05. n.s.=not significant.

Supplementary Figure 5

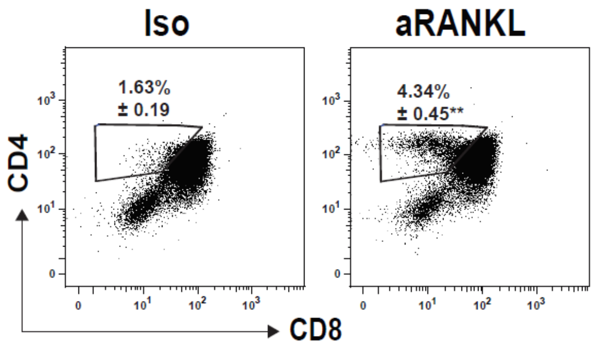

Supplementary Figure 5: anti-RANKL antibody impairs negative selection of TRP-1 specific CD4+ single positive T cells. Representative flow cytometric plots of CD4+ and CD8+ thymocytes from TRP-1 TCR Tg mice treated with isotype control antibody (iso) or anti-RANKL antibody (aRANKL). Mean +/- SD shown. t-test. **p<.01.

Supplementary Figure 6

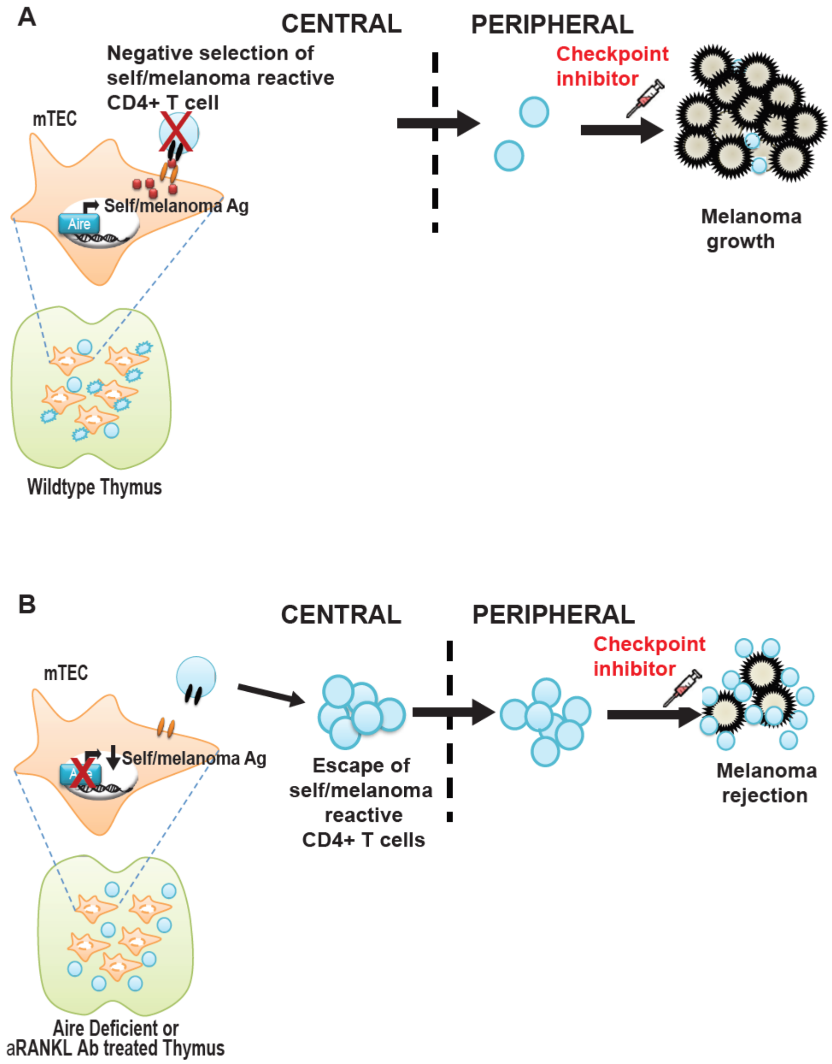

Supplementary Figure 6: Model of mechanism underlying additive anti-melanoma effects of combination central and peripheral tolerance blockade. A) In the thymus, Aire in mTECs promotes self/melanoma antigen expression, which results in negative selection of self/melanoma-reactive CD4^{+} T cells. As a result, the efficacy of checkpoint inhibition is limited by the scarcity of melanoma-reactive T cells in the periphery. B) Aire deficiency or transient depletion of Aire-expressing mTECs with anti-RANKL (aRANKL) antibody rescues self/melanoma antigen-reactive effector CD4^{+} T cells from negative selection. This expansion of the melanoma-reactive T cell pool available for activation by checkpoint inhibitors enhances anti-melanoma immunity.